Induction and suppression of NF-B signalling by a DNA virus of Drosophila

Induction and suppression of NF-κB signalling by a DNA virus of *Drosophila*

William H. Palmer[1,2*], Joep Joosten[3], Gijs J. Overheul[3], Pascal W. Jansen[4], Michiel Vermeulen[4], Darren J. Obbard[1,2], Ronald P. Van Rij[3*]

[1] Institute of Evolutionary Biology, University of Edinburgh, Kings Buildings, Charlotte Auerbach Road, Edinburgh, UK

[2] Centre for Infection, Evolution and Immunity, University of Edinburgh, Kings Buildings, Charlotte Auerbach Road, Edinburgh, UK

[3] Department of Medical Microbiology, Radboud University Medical Center, Radboud Institute for Molecular Life Sciences, P.O. Box 9101, 6500 HB Nijmegen, The Netherlands.

[4] Department of Molecular Biology, Faculty of Science, Radboud Institute for Molecular Life Sciences, Radboud University Nijmegen, 6525 GA Nijmegen, The Netherlands

*Authors for correspondence: W.H.Palmer@sms.ed.ac.uk; Ronald.vanRij@radboudumc.nl

Running title: NF-κB interactions with a *Drosophila* DNA virus

Abstract

Interactions between the insect immune system and RNA viruses have been extensively studied in *Drosophila*, where RNA interference, NF-κB and JAK-STAT pathways underlie antiviral immunity. In response to RNA interference, insect viruses have convergently evolved suppressors of this pathway that act by diverse mechanisms to permit viral replication. However, interactions between the insect immune system and DNA viruses have received less attention, primarily because few *Drosophila*-infecting DNA virus isolates are available. Here, we use a recently-isolated DNA virus of *Drosophila melanogaster*, Kallithea virus (family *Nudiviridae*), to probe known antiviral immune responses and virus evasion tactics in the context of DNA virus infection. We find that fly mutants for RNA interference and Immune deficiency (Imd), but not Toll, pathways are more susceptible to Kallithea virus infection. We identify the Kallithea virus-encoded protein gp83 as a potent inhibitor of Toll signalling, suggesting that Toll mediates antiviral defense against Kallithea virus infection, but that it is suppressed by the virus. We find that Kallithea virus gp83 inhibits Toll signalling through the regulation of NF-κB transcription factors. Furthermore, we find that gp83 of the closely related Drosophila innubila nudivirus (DiNV) suppresses *D. melanogaster* Toll signalling, suggesting an evolutionary conserved function of Toll in defense against DNA viruses. Together, these results provide a broad description of known antiviral pathways in the context of DNA virus infection and identify the first Toll pathway inhibitor in a *Drosophila* virus, extending the known diversity of insect virus-encoded immune inhibitors.

Importance

Co-evolution of multicellular organisms and their natural viruses may lead to an intricate relationship in which host survival requires effective immunity, and virus survival depends on evasion of such responses. Insect antiviral immunity, and reciprocal virus immune suppression tactics, have been well-studied in *Drosophila melanogaster*, primarily during RNA, but not DNA, virus infection.

Therefore, we describe interactions between a recently-isolated *Drosophila* DNA virus (Kallithea virus - KV) and immune processes known to control RNA viruses, such as RNAi and Imd pathways. We find that KV suppresses the Toll pathway, and identify gp83 as a KV-encoded protein that underlies this suppression. This immunosuppressive ability is conserved in another nudivirus, suggesting the Toll pathway has conserved antiviral activity against DNA nudiviruses, which have evolved suppressors in response. Together, these results indicate that DNA viruses induce and suppress NF-κB responses, and advance the application of KV as a model to study insect immunity.

Introduction

Innate antiviral immunity in insects has been best studied in response to RNA virus infections of *Drosophila melanogaster*. Antiviral immune mechanisms that target RNA viruses include RNA-mediated defences such as RNA interference (RNAi) and RNA decay pathways, cellular defences such as apoptosis, phagocytosis, and autophagy, and other effectors of resistance and tolerance that are transcriptionally induced following infection. The latter are primarily mediated by Janus kinase/signal transducers and activators of transcription (JAK-STAT) and Nuclear factor κB (NF-κB) pathways (reviewed in (1–5).

The insect response to DNA viruses is less well studied, but RNAi and apoptosis have demonstrated antiviral activity (6–8) and the JAK-STAT pathway is active during infection, possibly mediating a tolerance response (9). Baculovirus, nudivirus, and iridovirus infections of *Drosophila* all give rise to virus-derived small interfering RNA (vsiRNAs), which regulate DNA virus gene expression (7, 8, 10, 11) and mutants for RNAi effectors *Dicer-2* (*Dcr-2*) and *Argonaute-2* (*AGO2*) are hypersensitive to Invertebrate iridescent virus 6 (IIV6; an iridovirus) infection. This suggests that RNAi is also an important defence against DNA viruses, and IIV6 correspondingly encodes a suppressor of RNAi (7, 12). Virus-encoded suppressors of apoptosis are also widespread in DNA viruses, acting through binding and inhibition of cellular caspases (e.g. p35), or stabilization of cellular inhibitors of apoptosis (e.g. IAP gene family; (13–15)). In contrast, the contribution of transcriptional responses, such as the NF-κB pathways, to DNA viruses has not yet been elucidated.

There are two NF-κB pathways in *Drosophila*: Toll and Imd, which primarily function in antibacterial (Toll: gram-positive, Imd: gram-negative) and antifungal (Toll) defense, although both provide protection against some RNA viruses (reviewed in (1, 4, 5, 16, 17)). Toll and Imd pathways are activated following recognition of a pathogen-associated molecular patterns (PAMP; e.g. bacterial peptidoglycan), leading to the phosphorylation and degradation of the inhibitor of kappa B (IκB; encoded by *cactus* for Toll signalling, and by the *relish* C-terminus in Imd signalling) (reviewed in (16,

17). Under non-signalling conditions, IκB sequesters NF-κB transcription factors in the cytoplasm. These transcription factors are encoded by *dorsal* (*dl*) and *Dorsal immune-related factor* (*Dif*) in Toll signalling, and *Relish* (*Rel*) in Imd signalling, and all translocate to the nucleus to induce gene expression following IκB degradation (reviewed in (16, 17). Although the mechanism by which Toll and Imd recognise RNA viruses is unclear, both are active and provide immunity against some viral infections in insects, most likely through induction of antiviral effector responses. For example, Toll is broadly antiviral against RNA viruses such as Drosophila C virus, Nora virus, and Flock House virus in *Drosophila* during orally acquired, but not systemic infections, and in *Aedes* mosquitoes against dengue virus (18–21). Additionally, Imd is antiviral against a subset of viruses in *Drosophila*, such as Cricket Paralysis virus, Drosophila C virus, and Sindbis virus and in *Aedes* cell culture against the alphaviruses Semliki Forest virus and O'nyong'nyong virus (22–26).

Although the effect of NF-κB signalling on DNA virus infection in insects has not been directly tested, polydnaviruses, ascoviruses, baculoviruses, and entomopoxviruses have acquired suppressors of NF-κB signalling by horizontal gene transfer, providing indirect evidence for anti-DNA virus activity of NF-κB pathways (27, 28). First, a 'polydnavirus' encoded in the genome of the Braconid parasitoid wasp *Microplitis demolitor* has acquired homologs of IκB, some of which inhibit Dif and Rel by direct binding (27). However, this is a domesticated endogenous viral element that forms viral particles injected into the parasitoid's host, and as these IκB homologues are not found in related nudiviruses, baculoviruses, or hytrosaviruses, it seems likely that they were acquired to inhibit anti-parasitoid immune responses in the host of the parasitoid wasp, rather than the antiviral immune response of the wasp itself (29, 30). Second, homologs of *diedel*, which encode a cytokine that inhibits apoptosis and the Imd pathway in *Drosophila*, are similarly found in ascoviruses, baculoviruses, and entomopoxviruses, likely through independent horizontal transfer from arthropod hosts (28). Virus-encoded *diedel* phenocopies fly-encoded *diedel*, suggesting that viral diedel has retained an Imd-suppressive function, and that the Imd pathway likely interacts with these DNA viruses (28, 31). However, it is still unclear whether antiviral Toll signalling is targeted by insect virus-encoded

immune suppressors, and whether these hijacked host pathway inhibitors represent a subset of a greater diversity of NF-κB immune inhibitors or reflect evasion of virus-specific immune mechanisms.

The recent isolation of Kallithea virus (KV; (11, 32), a nudivirus that naturally infects *Drosophila melanogaster* at high prevalence in the wild, provides a tractable system to study host-DNA virus interactions and to identify immune evasion strategies in DNA viruses. Nudiviruses are large dsDNA viruses (100-200 kilobases, encoding roughly 100-150 genes) that most often infect the arthropod midgut and fat body and are transmitted faecal-orally (33–39). Because some virus-encoded immune suppressors have been found to be highly host-specific, the use of native host-virus pairs is vital to our understanding of viral immune evasion (e.g. (40–45). Here, we use this system to analyze the interaction between antiviral immune pathways and a DNA virus in *Drosophila*. Using mutant fly lines, we find that the RNAi and Imd pathways mediate antiviral protection against KV *in vivo*, but that abrogation of Toll signalling has no effect on virus replication. Through re-analysis of previous RNA-sequencing data, we observe a broad downregulation of NF-κB responsive antimicrobial peptides following KV infection and perform a small-scale screen for KV-encoded immune inhibitors. We identify viral protein gp83 as having a complex interaction with NF-κB signalling, leading to induction of Imd signalling but potent suppression of Toll signalling. This suppression acts directly through, or downstream of, NF-κB transcription factors. Finally, through analysis of the related Drosophila innubila nudivirus (DiNV) gp83 ortholog, we show that the immunosuppressive activity of gp83 against *D. melanogaster* NF-κB signalling is conserved.

Materials and Methods

Fly strains, virus growth, and mortality experiments

All fly lines were maintained and crossed on standard cornmeal medium at 25 °C. Viral titre and mortality were measured following KV infection in two control lines (w^{1118} and *Oregon R*) and in mutant lines compromised in the following immune signalling pathways: RNAi ($Dcr\text{-}2^{L811fsX}$ (46) and $AGO2^{414}$ (47)), Toll (spz^{4} (48), dl^{1} (49), and pll^{2}/pll^{21} trans-heterozygotes (51, 52)), and Imd (rel^{e20} (53) and imd^{10191} (54)).

For mortality assays, 100 female flies of each genotype were injected with 50 nL of either KV suspension (10^{5} ID_{50}, as described in (32)) or chloroform-treated KV suspension (which inactivates KV through the destruction of the membrane, (32)). For chloroform treatment, the KV suspension was mixed with an equal volume of chloroform, vortexed for 30 seconds, centrifuged for 5 minutes at 6000xg, and the aqueous phase was taken for downstream experiments. Injected flies were transferred to sucrose agar vials in groups of 10, and the number of surviving flies was recorded daily. While maintenance of flies on a protein-free diet likely affects some aspects of the immune response, we have assumed this is similarly tolerated across the fly lines used. Each group of flies was transferred to fresh food each week. Per-day mortality was analysed as a binomial response variable with the Bayesian generalised linear mixed modelling R package, MCMCglmm (55), with days post-inoculation (dpi), dpi^{2} (to allow for non-linear changes in mortality), and genotype as fixed effects, and vial as a random effect, as described previously (32). All confidence intervals are reported as 95% highest posterior density (HPD) intervals. All code used to fit the models described in this study, and associated data, are available on Figshare (doi: 10.6084/m9.figshare.c.4151009).

Viral titre was measured in each line after intra-abdominal injection of 50 nL of KV suspension. Infected female flies of each line (n=50) were transferred to 10 sucrose agar vials in groups of 5, and 5 vials of each genotype were homogenised in Trizol (Invitrogen) at 5 and 10 dpi. For RNAi mutants, flies were also assayed at 3 dpi. DNA was extracted by phenol-chloroform precipitation and viral titre estimated by quantitative PCR relative to host genomic DNA, using previously described primers (rpl32; (32)). Log-transformed viral titre was analysed as a Gaussian response variable using

MCMCglmm (55), with genotype, dpi, and genotype-by-dpi interactions as fixed effects. Titre in RNAi and NF-κB mutants were assayed in separate experiments, and therefore analysed independently. A statistical approach was used to account for the impact of differing genetic backgrounds between mutant lines, using the range of KV titres seen previously across 120 different natural genetic backgrounds from the *Drosophila* Genetic Reference Panel (32). Specifically, considering w^{1118} and *Oregon R* as controls and mutants of each pathway as the 'experimental' group, a null distribution of effect sizes expected only from differences in genetic background was created by randomly choosing two DGRP lines to serve as controls and additional DGRP lines reflecting the mutant lines used in each pathway. For each null draw, the same model was fitted as described above, the absolute value of the effect size was recorded, and this was repeated 1000 times to obtain a distribution. If the average effect size associated with mutants in a pathway was greater than the highest 5% of effect sizes, we concluded that the observed differences in KV titre were due to mutations in the tested pathway.

Cell culture and virus propagation

S2 cells (Invitrogen) were cultured at 25 °C in Schneider's Drosophila Medium with 10% heat-inactivated fetal bovine serum and 50 U/mL penicillin and 50 ug/mL streptomycin (Life technologies). KV was purified from flies 10 days after initial infection as previously described (32). Briefly, KV was injected into 2000 *Oregon R* adult flies, which were incubated at 25 °C for 10 days, homogenised in 5 mL 10 mM Tris-HCl, filtered through cheese cloth, centrifuged twice for 10 minutes at 6000xg, filtered through a 0.22 µm polyvinylidene fluoride syringe filter, and subject to gradient centrifugation in an iodixanol (Optiprep) gradient (32). KV-positive fractions of the gradient, as assessed by qPCR, were kept as the KV isolate. To measure the effects of KV on cell size and number, $5x10^4$ S2 cells were seeded in 96-well plates, followed by the immediate addition of 5 µL of either KV suspension (10^3 ID_{50}) or chloroform-treated KV. Cells were split once 7 dpi, and cell size and number was measured using FIJI 10 dpi (56).

Cloning

We selected 9 KV genes identified as highly expressed at three dpi (32) to screen for KV-encoded immune suppressors. These were *gp23, gp43, gp83, ACH96233.1-like, ACH96143.1-like, putative protein 1, putative protein 12, putative protein 15, putative serine protease* (corresponding to GenBank accession numbers AKH40365.1, AKH40394.1, AKH40369.1, AKH40392.1, AKH40340.1, AQN78560.1, AKH40392.1, AKH40404.1, and AQN78556.1). Each KV gene was amplified using the Qiagen Long Range PCR kit as per the manufacturer's instructions, with primers that introduced restriction sites and the *Drosophila* Kozak sequence (restriction enzymes and primers used in (Table 1), and cloned into a pAc5.1 vector (Invitrogen) with a C-terminal V5-His tag. The KV gene *gp83* was also cloned into pAc5.1 vector with GFP instead of V5-His to introduce a C-terminal GFP tag. Deletion constructs for gp83 were created by separately amplifying 2 segments of gp83 with primers that span the desired deletion and performing a second PCR reaction with these segments as a template, and the forward and reverse primers from the 5' and 3' segments, respectively (Table 1; gp83$^{\Delta 1}$: CGLIECSELLRDRLCSKL deletion; gp83$^{\Delta 2}$: WSDRLNLI deletion). The resulting amplicons with deletions were cloned as described above. The *gp83* gene from DiNV (35, 57) was also cloned as above (Table 1).

Additionally, Toll pathway components *pll*, *tube, cact, Dif*, and *dl* were cloned into the pAc5.1 vector, as described above (Table 1). Other Toll and Imd pathway constructs have been described before: pAc5.1-Toll^{LRR} (58), pAc5.1-dl-GFP (59), pMT-PGRP-LCx (60), pAc5.1-rel-GFP (61), and the firefly luciferase (FLuc) reporter plasmids with promoter sequences from *Drosomycin* (*Drs*), *Diptericin* (*Dpt*), and *Attacin-A* (*Att-A*) (58) or with 10X STAT binding sites (62).

Transfection and RNAi Knockdown in S2 cells

S2 cells were transfected using Effectene transfection reagent, as per the manufacturer's instructions. Double-stranded RNA (dsRNA) was synthesized against *cactus*, *gp83*, *FLuc*, *renilla luciferase* (*RLuc*), and *GFP* for RNAi-mediated knockdown. Primers with flanking T7 sequences were

198 used to amplify regions of each gene (Table 1) and dsRNA was synthesized from the resulting PCR
199 products with T7 RNA polymerase and purified using GenElute Total RNA mini kit (Qiagen) (63).

200 *Immune suppression assays*

201 The 9 cloned KV genes were tested for their ability to suppress RNAi, JAK-STAT, Toll, or Imd activity.
202 RNAi suppression assays were performed as described previously (63). Briefly, $5x10^4$ S2 cells were
203 seeded in a 96-well plate and 24 hours later transfected with 33 ng of pMT-FLuc, 33 ng pMT-Rluc,
204 and 33 ng of either pAc5.1 empty vector or the pAc5.1 expression plasmid encoding a KV gene. Two
205 days later, 400 ng of either GFP or FLuc dsRNA was added to each well, and $CuSO_4$ was added 8
206 hours later to a final concentration of 500 μM to induce expression of the luciferase reporters. RLuc
207 and FLuc luciferase activity were measured using the Dual Luciferase Assay Kit (Promega).

208 For JAK-STAT immunosuppression assays, $5x10^4$ S2 cells were seeded in a 96-well plate and
209 transfected 24 hours later with 30 ng of 10XSTAT-FLuc, 20 ng pAc5.1-Rluc, and 50 ng of either pAc5.1
210 empty vector or the pAc5.1 expression plasmid encoding a KV gene. Luciferase activity was
211 measured at 48 hours following transfection.

212 For NF-κB immunosuppression assays, a plasmid encoding the Imd receptor PGRP-LC (isoform x;
213 pMT-PGRP-LCx) (60, 64) or a constitutively active Toll construct lacking the extracellular leucine-rich
214 repeat domain, pAc5.1-Toll^{LRR} (58) was transfected alongside each KV gene, and a NF-κB-responsive
215 FLuc reporter containing either the *Dpt* (Imd) or *Drs* (Toll) promoter sequence (58). For Toll immune
216 suppression assays, $5x10^4$ S2 cells were seeded in 96-well plates and 24 hours later transfected with
217 50 ng of either empty pAc5.1 vector or a pAc5.1 KV gene expression construct, 20 ng of either
218 pAc5.1 or pAc5.1-Toll^{LRR}, 10 ng of Drs-FLuc, and 10 ng pAc5.1-Rluc. Imd immune suppression assays
219 were performed in the same manner, except that pMT, pMT-PGRP-LCx, and Dpt-FLuc were
220 substituted for pAc5.1, pAc5.1-Toll^{LRR}, and Drs-FLuc, respectively, and $CuSO_4$ was added immediately
221 following transfection. Analogous experiments were performed using pAc5.1-dl, pAc5.1-Dif, and
222 pAc5.1-pll instead of pAc5.1-Toll^{LRR}, or by transfecting 5 ng of *cact* dsRNA. In the latter case, 70 ng of

KV gene expression construct was transfected instead of 50 ng. RLuc and FLuc activity were assayed 48 hours after transfection.

Immunosuppression assays were also performed using KV-infected cells. $5x10^4$ cells were seeded in 96-well plates, followed by the immediate addition of 5 µL of either KV suspension (10^3 ID_{50}) or chloroform-treated KV, and transfected the next day. For RNAi suppression assays with KV, 50 ng pMT-RLuc, 50 ng pMT-FLuc (63), and 5 ng of either GFP or GL3 dsRNA were transfected 2 dpi and $CuSO_4$ added 8 hours later. To measure JAK-STAT activity following KV infection, 70 ng of 10XSTAT-FLuc and 30 ng pAc5.1-Rluc (65) were transfected. For Toll suppression assays, 70 ng of either pAc5.1 or pAc5.1-$Toll^{LRR}$, 20 ng of Drs-FLuc, and 10 ng pAc-RLuc were transfected. Finally, to measure Imd activity following KV infection, 70 ng of either pMT or pMT-PGRP-LCx, 20 ng of Dpt-FLuc, and 10 ng pAc-RLuc were transfected, and $CuSO_4$ was added immediately following transfection. Luciferase activity was measured at 4 dpi.

The R package MCMglmm was used to determine significance in immune suppression assays, with the RLuc-normalised FLuc values as a Gaussian response variable. In the original screen for immune suppressors, any experimental induction of an immune pathway was treated as a fixed effect (e.g. addition of dsRNA against FLuc in the RNAi suppression assay, PGRP-LC overexpression in the Imd suppression assay, and $Toll^{LRR}$ transgene expression in the Toll suppression assay), each KV gene was treated as a random effect, and the interaction between KV gene and the induced experimental change to signalling output was treated as a random effect. In subsequent NF-κB suppression experiments, where the only tested KV gene was gp83, gp83 and the interaction between gp83 and overexpression of NF-κB receptors were treated as fixed effects. Likewise, when immune suppression experiments were carried out with KV-infected cells instead of cells expressing individual KV transgenes, KV infection status, the induction of an immune pathway, and the interaction between these were treated as fixed effects.

Immunoprecipitation and western blotting

To test whether gp83 directly interacted with dl, $2x10^6$ S2 cells were seeded in 6-well plates and transfected with 150 ng of either pAc5.1 empty vector, pAc5.1 encoding V5-tagged gp83, or V5-tagged cact alongside 150 ng of the expression plasmid (pAc5.1) encoding GFP or GFP-tagged dl. Two days post-transfection, two wells per treatment were resuspended in lysis buffer (0.1% NP-40, 30 mM Hepes-KOH, 150 mM NaCl, 2mM MgOAc) supplemented with cOmplete protease inhibitor cocktail (Roche) and 5 mM DTT, and disrupted 30 times through a 25-gauge needle. After 10 minutes incubation on ice, cell debris was pelleted by centrifuging at 16,000xg for 30 minutes and supernatant was either stored as an input control or collected and incubated for 5 hours at 4 °C with magnetic control beads. Binding control beads were removed and the resulting supernatant was incubated with GFP-trap magnetic beads (Chromotek) overnight at 4 °C. Beads were washed 3 times in lysis buffer and 3 times in 25 mM Tris-HCl, 150 mM NaCl solution, and protein complexes eluted by boiling 10 minutes at 95 °C in Laemmli buffer.

Whole cellular protein extracts were prepared by heating S2 cells for 10 min at 95 °C in Laemmli buffer. Whole cellular extracts or immunoprecipitated proteins were separated on a 12% SDS-PAGE gel and transferred to a nitrocellulose membrane. Non-specific binding was blocked with blocking solution (phosphate buffered saline with 0.1% Triton-X (PBT) and 5% dry milk). Proteins of interest were probed with primary antibody diluted in blocking solution overnight at 4 °C, and visualized with an hour incubation of secondary antibody in blocking solution. Membranes were washed 3 times in PBT before and after each step. The following antibodies were used: mouse anti-dl (1:100 dilution, Developmental Studies Hybridoma Bank), mouse anti-V5 (1:1000 dilution, Invitrogen), rat anti-tub-α (1:1000 dilution, SanBio), and rabbit anti-GFP (1:1500 dilution, abcam ab6556) as primary antibodies, and goat anti-mouse IR-Dye 680 (1:15,000 dilution, LI-COR), goat anti-rat IR-Dye 800 (1:15,000 dilution, LI-COR), goat anti-rabbit IR-Dye 800 (1:15,000, LI-COR). An Odyssey Infrared Imager (LI-COR) was used to image blots.

Mass spectrometry

10^6 S2 cells were co-transfected with pCoBLAST and pAc5.1-gp83^{GFP} plasmid at a 1:19 ratio (125 ng and 2.38 µg, respectively). Medium was replaced 3 hours post-transfection, and again at 48 hours post-transfection with medium supplemented with blasticidin (20 µg/mL). Another 48 hours later, cells were refreshed with medium containing 4 µg/mL blasticidin, which was thereafter replaced every 3-4 days with medium containing 4 µg/mL blasticidin, resulting in a polyclonal cell line.

For mass spectrometry, wild-type S2 cells or S2 cells stably expressing GP83^{GFP} were lysed in 50mM Tris-HCl (pH 7.8), 150mM NaCl, 1% NP-40, 0.5mM DTT, 10% glycerol, and protease inhibitor cocktail (Roche). Approximately 4 mg of protein lysate was subjected to GFP-affinity purification using 7.5 µL GFP-trap beads (Chromotek) for approximately 1.5 hours at 4 °C. Beads were washed twice in lysis buffer, twice in PBS containing 1% NP-40, and three times in PBS, followed by on-bead trypsin digestion as described previously (66). Afterwards, tryptic peptides were acidified and desalted using Stagetips, eluted, and brought onto an EASY-nLC 1000 Liquid Chromatograph (Thermo Scientific). Mass spectra were recorded on a QExactive mass spectrometer (Thermo Scientific) and MS and MS2 data were recorded using TOP10 data-dependent acquisition. Maxquant (v1.5.1.0) was used to analyse raw data, using recommended settings (67). LFQ, IBAQ, and match between runs were enabled. The peptides were mapped to *D. melanogaster* proteins (UniProt June 2017) and contaminants and reverse hits were filtered with Perseus (v1.3.0.4) (68). Missing values were imputed, assuming a normal distribution, and significance determined by a t-test on log-transformed LFQ-values between wild-type and gp83-expressing S2 cells.

Immunofluorescence microscopy

$5x10^5$ S2 cells were seeded in 12-well plates with glass coverslips in each well. Cells were transfected with 100 ng of pAc5.1 or pAc5.1-gp83-V5 and 100 ng of pAc5.1-dl-GFP. Two days after transfection, cells were fixed with 4% paraformaldehyde, washed twice in PBS, once with PBT, and blocked with PBT with 10% goat serum. Cells were stained by incubation with mouse anti-V5 (1:400, Invitrogen) for one hour, followed by fluorophore-containing goat anti-mouse secondary antibody (1:400,

AlexaFluor) with 10 ug/mL Hoechst for one hour. Finally, cells were washed twice in PBT and twice in PBS, mounted on slides with Fluoromount-G (eBiosciences), and imaged with an Olympus FluoView FV1000. Fluorescence was measured in whole cells, or separately in the cytoplasm and nuclei by outlining the region of interest in Fiji (56) to calculate the mean fluorescence.

Data availability

All data presented in this manuscript, and associated code to fit statistical models, is provided via Figshare (doi: 10.6084/m9.figshare.c.4151009).

Results and Discussion

RNAi and Imd pathways are antiviral against KV in vivo

The RNAi pathway provides antiviral activity against the DNA virus IIV6, and KV-derived vsiRNAs are produced upon infection of adult naturally-infected *Drosophila* (7, 11, 12). However, the contribution of Imd and Toll pathways to anti-DNA virus immunity have not been described. We used fly lines mutant for RNAi, Imd, and Toll pathway components to assess whether these pathways fulfil an antiviral function during KV infection. First, we infected mutants for RNAi genes *Dcr-2* and *AGO2* with KV, and measured viral titre and mortality following infection. Following KV infection, both *Dcr-2* and *AGO2* mutants exhibited significantly greater KV titres at 3 dpi, with KV titre 78-fold greater in *Dcr-2* mutants (95% HPD intervals: 18-281 fold; MCMCp < 0.001) and 55-fold greater in *AGO2* mutants (13-237 fold, MCMCp < 0.001; Figure 1A). However, the increased KV replication in RNAi mutants was not sustained at later infection timepoints. At 5 dpi, *Dcr-2* mutants did not have significantly different KV titre from the controls (MCMCp = 0.22), but titres were still increased in *AGO2* mutants, albeit to a lesser extent that at 3 dpi (12-fold increase; 2.5-43 fold, MCMCp < 0.001; Figure 1A). By 10 dpi, there was no significant difference between viral titre in control flies and either *Dcr-2* mutants (MCMCp = 0.43) or *AGO2* mutants (MCMCp = 0.7). Therefore,

either the antiviral effect of RNAi is short-lived (for example, a viral suppressor of RNAi may eventually be expressed *in vivo*), other immune pathways take over as the dominant antiviral force, or KV negatively regulates its own replication or depletes a resource. Nevertheless, despite the similar titres during late infection, there was still a significant increase in KV-induced mortality in *Dcr-2* and *AGO2* mutants, where 70% of control flies were alive at 19 dpi, compared to 25% in *Dcr-2* mutants (MCMCp = 0.014) and 38% in *AGO2* mutants (MCMCp = 0.004, Figure 1B). Increased late life mortality in RNAi mutants could be due to early host damage or to increased expression of virulence factors throughout infection, expression of which could be regulated by RNAi, independent of KV titre (e.g. (10). These results extend the antiviral role of the RNAi pathway to KV infection.

We next infected Imd and Toll pathway mutants with KV and assessed KV DNA levels by qPCR at 5 and 10 dpi. We found that Imd pathway mutants had significantly greater viral titre as compared to two control lines, with *imd* mutants having 6-fold greater KV titre at 5 and 10 dpi (2.7-13.7 fold, MCMCp < 0.001), and *Rel mutants* having 8-fold greater viral titre at 5 and 10 dpi (3.1-15.9 fold, MCMCp < 0.001; Figure 1C). Because the Imd effect spans 5 and 10 dpi, and we have previously measured KV titre in 125 inbred lines of the *Drosophila* Genetic Reference Panel at 8 dpi (32, 69), we attempted to account for genetic background by comparing the average effect of Imd mutants to the distribution of effects consistent with natural variation in the genetic background. This analysis indicated that the increased titre observed in Imd mutants is unlikely to be due to genetic background (p = 0.01). We also infected flies mutant for the Toll pathway components *spz*, *pll*, and *dl.* Viral titre was unchanged in Toll pathway mutants compared to controls, and the pathway-level effect of Toll mutants was within the expected distribution of effects caused by differences in genetic background (p = 0.28). We conclude that the Imd pathway is antiviral against KV, but that abrogation of Toll function has no effect on KV growth. This could indicate that Toll is not antiviral against this DNA virus, or that the pathway is efficiently suppressed by virus infection. The latter is consistent with our observation that genes encoding antimicrobial peptides are generally downregulated in KV-infected flies compared to uninfected controls (Figure 1E), and we therefore

explored the capability of KV to suppress innate immune pathways using a cell culture model of immunosuppression.

KV replicates efficiently in some Drosophila cell lines

To establish a cell culture model for KV infection, we analyzed viral replication in five commonly-used *D. melanogaster* cell lines. We found variation in the ability of KV to infect these cells, with efficient replication in several *Drosophila* S2 cell clones, including S2 (not shown), S2R+, and DL2 cells, but no or inefficient replication in Kc167 and Dm-BG3-c2 cells (Figure 2A). In S2 cells, which we used for further analyses, KV was released into the medium at substantial levels starting from 3 dpi (Figure 2B). Therefore, in all subsequent experiments, we assayed cells at 4 dpi, assuming that a high proportion of cells would be infected at this timepoint. We did not observe any overt cytopathic effects of KV-infected cells within 14 days of infection. However, when KV-infected cells were passaged at 7 dpi, we observed larger (MCMCp < 0.001) and fewer (MCMCp < 0.001) cells, likely due to a decrease in cell proliferation (Figure 2C,D).

KV leads to downregulation of JAK-STAT and Toll, and induction of Imd signalling in cell culture

We used previously established luciferase reporter-based assays to describe the effect of KV infection on RNAi, JAK-STAT, Toll, and Imd pathways in cell culture. To determine if KV suppresses RNAi, we measured the RNAi silencing efficiency of cells inoculated with KV or chloroform-inactivated KV (hereafter referred to as mock-treated) by co-transfecting an expression plasmid encoding FLuc with either GFP dsRNA or FLuc dsRNA. In both mock and KV-treated cells, FLuc dsRNA caused a 95% reduction in FLuc activity compared with GFP dsRNA treated cells, indicating that KV infection does not inhibit RNAi in cell culture (MCMCp = 0.9; Figure 3A). Many viruses studied in *Drosophila* encode a suppressor of RNAi (e.g. (12, 44, 65, 70–73), and therefore the absence of KV-induced RNAi suppression is somewhat surprising. It is possible that KV-RNAi interactions are different in the cell types that are naturally infected by KV, and that our inability to observe RNAi suppressive activity is a limitation of the cell culture model. Alternatively, if KV transmission does not

occur until later stages of infection, there may be limited selective pressure to evade RNAi, as RNAi mutants and control flies have similar titres during late infection.

The JAK-STAT pathway has an antiviral role during Drosophila C virus infection (74) and mediates tolerance to the DNA virus IIV6, evidenced by upregulation of *vir-1* and *Turandot* (*Tot*) genes (9). However, previous *in vivo* transcriptional profiling did not identify strong differential expression of STAT-responsive genes following infection with KV (Figure 1E) (32). We assessed JAK-STAT activity in mock and KV-treated cells with a FLuc reporter driven by a promoter containing ten STAT binding sites (62). This reporter is endogenously active in S2 cells (62), but KV infection led to a 58% reduction in STAT-mediated FLuc activity (37-74%, MCMCp < 0.001; Figure 3C), indicating that JAK-STAT is down-regulated or inhibited following KV infection. However, in addition to mediating a transcriptional immune response, the JAK-STAT pathway is involved in cell proliferation (75), which also decreases following KV infection in cell culture (Figure 2), making cause and effect difficult to distinguish.

We next assayed the effect of KV on Toll and Imd signalling. However, these pathways are not constitutively active in S2 cells. To measure KV suppression of these pathways, we therefore co-transfected $Toll^{LRR}$ (a Toll receptor lacking the leucine-rich repeat extracellular domain) or PGRP-LC (an Imd pathway receptor) with *Drs* or *Dpt* luciferase reporters to artificially induce signalling of Toll and Imd pathways, respectively. Transfection of $Toll^{LRR}$ increased Drs-Fluc by 243-fold (MCMCp < 0.001), consistent with previous reports (58). However, KV infection reduced the maximum level of $Toll^{LRR}$-mediated Drs activity by 81% (38-93%, MCMCp < 0.001; Figure 3E), indicating KV can inhibit Toll signalling. Over-expression of PGRP-LC led to a 4-fold increase in Dpt-FLuc (3-5 fold, MCMCp < 0.001). In contrast to the effect on Toll signalling, KV infection led to a 3.6-fold increase (2.6-4.8 fold, MCMCp < 0.001) in Dpt-FLuc, which additively increased when PGRP-LC overexpressing cells were infected with KV (17-fold increase compared to Imd-inactive, mock-treated cells; 12-23 fold, Figure

3G). These results suggest that KV infection in S2 cell culture leads to downregulation or suppression of Toll signalling but induction of Imd signalling.

KV-encoded gp83 modifies NF-κB signalling during infection

The immunosuppressive function of nudivirus genes has not previously been explored. Because we observe KV-mediated downregulation of NF-κB-regulated AMPs *in vivo* and downregulation of JAK-STAT and Toll reporters *in vitro*, we wished to identify potential KV-encoded suppressors of canonical immune pathways. Therefore, we cloned 9 uncharacterized KV genes that are highly expressed at 3 dpi in adult flies (32) and performed immune suppression assays for RNAi, JAK-STAT, Toll, and Imd pathways. We were unable to identify KV-encoded suppressors of RNAi or JAK-STAT among these 9 genes, although we confirmed that Cricket Paralysis Virus protein 1A potently suppressed RNAi in these assays, as expected ((72); MCMCp = 0.006; Figure 3B,D). However, we found that gp83—a KV gene encoding no recognisable protein domains, named for its homology to the Gryllus bimaculatus nudivirus (GbNV) gp83 locus (76)—significantly reduced $Toll^{LRR}$-dependent Drs-FLuc expression (Figure 3F). In this experiment, $Toll^{LRR}$ expression induced Drs-FLuc by 24-fold (8-66 fold), but by only 1.9-fold (0.3-8 fold; MCMCp = 0.02) when gp83 was co-expressed. We further found that expression of gp83 caused a 5-fold (1.5-18 fold) *increase* in Imd-mediated Dpt-FLuc expression, with or without PGRP-LC overexpression (MCMCp = 0.008; Figure 3H).

We next aimed to confirm that the interactions between the transfected KV gene gp83 and NF-κB pathways are representative of the function of gp83 during KV infection. Therefore, we silenced gp83 during KV infection using dsRNA, and measured associated changes in Toll, Imd, and JAK-STAT signalling. Co-transfection of gp83 with independent dsRNAs targeting gp83 completely reversed inhibition of Drs-FLuc compared with transfection of GFP dsRNA, indicating that these dsRNAs effectively silence gp83 (MCMCp < 0.001 for both dsRNAs; Figure 4D). As reported above (Figure 3E), KV infection had no effect on Drs-FLuc in the absence of $Toll^{LRR}$ (MCMCp = 0.26), but inhibited $Toll^{LRR}$-induced signalling (MCMCp < 0.001). Knockdown of gp83 during KV infection of $Toll^{LRR}$-expressing

cells led to increased Drs-FLuc (MCMCp < 0.001; orange bars in Figure 4A). Surprisingly, Drs-FLuc was also slightly increased in Toll-inactive cells upon KV infection and gp83 knockdown (MCMCp = 0.004; grey bars in Figure 4A). Likewise, knockdown of gp83 in KV-infected cells expressing PGRP-LC caused a decrease in Dpt-FLuc expression (MCMCp = 0.006; orange bars in Figure 4B), and this effect was also noticeable in controls that do not express PGRP-LC (MCMCp = 0.03; grey bars in Figure 4B). Consistent with a specific interaction with NF-κB signalling, gp83 knockdown had no effect on the ability of KV to downregulate JAK-STAT signalling in S2 cells (MCMCp = 0.63; Figure 4C). Together, these observations indicate that gp83 is responsible for Toll suppression and Imd activation during KV infection.

The immunosuppressive function of gp83 on Toll signalling *in vitro* is consistent with the observed downregulation of AMPs following KV infection *in vivo* and substantiates the hypothesis that Toll is antiviral and suppressed during infection. However, the induction of antiviral Imd signalling by a single viral protein is unexpected, and it is unclear why KV has not evolved to avoid or suppress Imd activation as seen for other insect-infecting DNA viruses (28). Assuming that Imd activation is detrimental to virus transmission, this could indicate a trade-off between suppression of Toll and activation of Imd, or that gp83 is directly recognised by the fly immune system. Additionally, gp83-mediated Imd activation *in vitro* is at odds with the observed broad downregulation of AMPs *in vivo*, which are controlled, in part, by Imd signalling. This could be explained by differences in the intracellular versus systemic effects of KV on Imd signalling, or tissue-specific responses to KV, either of which could mask an excitatory effect of gp83 on Imd *in vivo*. Because of these inconsistencies, we chose to focus specifically on the Toll immunosuppressive effect of gp83, because the *in vitro* data is consistent with observed AMP expression patterns *in vivo*. We conclude that KV-encoded gp83 is involved in mediating complex interactions with NF-κB signalling *in vitro*, including suppression of Toll signalling and induction of Imd signalling.

Immune suppression by gp83 occurs downstream of Toll transcription factors

447 Previously described polydnavirus-encoded Toll pathway inhibitors imitate IκB, blocking the nuclear
448 entry of NF-κB transcription factors (27). Although the precise mechanism of interaction between
449 gp83 and Toll signalling is unknown, suppression of Toll^{LRR}-induced signalling indicates that gp83
450 functions downstream of Toll, and interferes with intracellular Toll signalling. We therefore
451 performed genetic interaction experiments between gp83 and downstream Toll components to
452 narrow down the point in the Toll signalling pathway at which gp83 acts. As observed before with
453 reporter assays, gp83 inhibited Toll^{LRR}-mediated signalling, now assessed by qRT-PCR of endogenous
454 *Drs* expression (MCMCp < 0.001; Figure 5A). Additionally, Drs-FLuc was greatly increased by
455 overexpressing *pll* (240-fold [131-414] induction of Drs-FLuc), silencing *cact* (75-fold [33-161]
456 induction of Drs-FLuc), overexpressing *Dif* (563-fold [317-1002] induction of Drs-FLuc;), and
457 overexpressing *dl* (459-fold [257-778] induction of Drs-FLuc;). Co-expression of gp83 potently
458 reduced Drs-FLuc in each of these scenarios (MCMCp < 0.001 for each) – pll/gp83 co-overexpression
459 led to a 0.55-fold change in Drs-FLuc (0.31-0.99 fold), cact^{dsRNA}/gp83 led to a 1.73-fold change in Drs-
460 FLuc (0.75-3.5 fold), Dif/gp83 led to a 0.86-fold change in Drs-FLuc (0.5-1.5 fold), and dl/gp83 led to a
461 1.5-fold change in Drs-FLuc (0.9-2.5 fold) relative to baseline Drs-FLuc expression (Figure 5B-E).
462 Additionally, V5 staining of V5 epitope-tagged gp83 revealed that gp83 is a nuclear protein (Figure
463 5F). Together, these results indicate that gp83 either inhibits NF-κB transcription factors, or acts
464 downstream of them to suppress Toll signalling *in vitro*.

465 Virus-encoded inhibitors of NF-κB in mammals have been reported to operate by promoting
466 degradation of NF-κB transcription factors, blocking NF-κB access to the nucleus, or interfering with
467 transcriptional co-activators to evade the interferon response (reviewed in 77). In order to better
468 define the mechanism of the immunosuppressive action of gp83, we searched for direct host
469 interactions that may mediate Toll suppression. Because our genetic interaction experiments
470 indicate that gp83 acts on or downstream of dl, we first tested for a physical interaction between dl
471 and gp83 using co-immunoprecipitation and subsequent western blotting. Following
472 immunoprecipitation of GFP-tagged dl, we were able to detect cact as an interacting positive

control, but we did not detect gp83 in GFP-dl immunoprecipitation (Figure 6C). Thus, to identify host interacting proteins of gp83 in an unbiased manner, we created an S2 cell line stably expressing GFP-tagged gp83, immunoprecipitated $gp83^{GFP}$, and performed quantitative mass spectrometry on interacting partners. We identified 19 *D. melanogaster* proteins, including 4 nuclear proteins (Nipped-B, Brf, Mlf, Ulp1), that were enriched in the gp83 immunoprecipitate (log_2 fold enrichment > 2.5; FDR < 0.1; Figure 6A). While we did not identify known downstream NF-κB pathway factors, the extracellular Toll ligand spz was enriched, despite the nuclear localization of gp83. However, peptide coverage of spz was poor and dsRNA knockdown of spz did not rescue the immunosuppressive effect of gp83, indicating that this interaction may not occur in live cells, or that it is not required for gp83 to inhibit Toll signalling (Figure 6B). Further, dsRNA-mediated knockdown of a subset of the enriched genes, including 3 of the 4 identified nuclear proteins, was unable to rescue the gp83 immunosuppressive effect (Figure 6B), suggesting that gp83 may not form stable complexes with host proteins to interfere with NF-κB signalling.

Although we did not detect a direct association between dl and gp83, we observed a reduction in dl protein levels upon gp83 overexpression that is not dependent on Toll signalling (Figure 7A). We quantified this effect by transfecting either GFP or GFP-tagged dl, in the absence or presence of gp83, and measuring fluorescence by confocal microscopy. We found that while gp83 caused a 53% reduction in GFP levels (42-62%, MCMCp < 0.001), possibly due to a dl binding site in the actin 5C promoter of this construct (78), gp83 caused a significantly greater reduction in dl^{GFP} (73% reduction; 66-78%, MCMCp < 0.001; Figure 7B,C). However, KV infection did not decrease dl protein levels, indicating that this may not be the primary mechanism by which KV inhibits Toll signalling (Figure 7A). Instead, we hypothesize that gp83 interferes with the access of dl to either the nucleus or to NF-κB binding sites, which indirectly affects dl localization and results in increased turnover. We prefer the latter explanation, that gp83 directly interferes with the Toll pathway transcriptional response, because overexpression of gp83 simultaneously induced the *Dpt* reporter (Figure 2H) and reduced dl-responsive promoters (Drs-FLuc and Act5C-GFP; Figure 3F, Figure 7B,C). These observations

implicate gp83 in regulating transcription at diverse loci responsive to both dl and Rel, and suggest an interaction between gp83 and NF-κB-responsive genes, possibly by directly interacting with DNA.

Immunosuppressive function of gp83 depends on conserved residues and is conserved in other nudiviruses

Conflict between the host immune system and virus-encoded immune inhibitors may result in an evolutionary arms race, leading to recurrent positive selection and eventual host specialization (e.g. (79–81). Consistent with this, some immune inhibitors are only effective against their native host species, thereby defining the viral host range (e.g. 40–45). We tested whether the immunosuppressive function of gp83 is conserved, and whether gp83 acts in a species-specific manner. The gp83 locus is absent from nudiviruses distantly related to KV, such as Heliothis zea nudivirus 1 (HzNV1), Tipula oleracea nudivirus (ToNV) and Peneaus monodon nudivirus (PmNV), but gp83 homologs are found in the more closely related GbNV, Nilaparvata lugens endogenous nudivirus (NlENV), Oryctes rhinoceros nudivirus (OrNV), Drosophila innubila nudivirus (DiNV), Tomelloso virus (TV), Mauternbach virus (MV), and Esparto virus (EV; Figure 8A). Although gp83 lacks recognisable protein domains, several regions are strongly conserved among these nudiviruses, suggesting functional conservation (Figure 8B). To test whether gp83 function depends on these conserved domains, we made two gp83 deletion constructs ($gp83^{\Delta1}$ and $gp83^{\Delta2}$) that remove conserved regions of respectively 18 and 8 amino acids without substantially altering protein stability, and transfected these alongside $Toll^{LRR}$ with the Drs-FLuc reporter. Although detectable by western blotting (Figure 8B), $gp83^{\Delta1}$ (MCMCp = 0.67) and $gp83^{\Delta2}$ (MCMCp = 0.79) were unable to inhibit Toll signalling, indicating that these conserved residues are important for the immunosuppressive function of gp83 (Figure 8C).

To test whether gp83 function is conserved among viruses, we cloned gp83 from DiNV, which has not been found to be associated with *D. melanogaster* (11), and performed Toll immunosuppression assays. The gp83 homolog from DiNV was able to completely inhibit *D. melanogaster* Toll signalling

in S2 cells (MCMCp < 0.001), despite only 57% amino acid identity with KV gp83, demonstrating that the immunosuppressive function of gp83 is conserved in other nudiviruses and that it is not highly host-specific (Figure 8D). This observation suggests that the Toll-gp83 interaction may not be a hotspot of antagonistic 'arms race' coevolution and has not led to specialization of DiNV gp83 to the *D. innubila* immune system at the expense of its ability to function in *D. melanogaster*. This could be because gp83 has relatively few direct interactions with host proteins (Figure 6A), and may instead interact directly with transcription factor binding sites which are under high constraint, and therefore unable to evolve resistance to the immunosuppressive effect of gp83 (82).

Conclusions

In this study we investigated the role of known anti-RNA viral immune pathways in the context of DNA virus infection, including RNAi, JAK-STAT, Imd, and Toll pathways. Our data support an antiviral role for RNAi and Imd against KV, consistent with previously-described antiviral RNAi against IIV6 and DNA virus-encoded suppressors of Imd (7, 8, 28). Furthermore, we identified gp83 as a KV-encoded Toll suppressor that acts downstream of NF-κB transcription factor release of IκB in cell culture, suggesting that Toll signalling can be antiviral during DNA virus infection in insects. The immunosuppressive effect of gp83 is conserved in other nudiviruses, and has not evolved host-specificity in DiNV, indicating that the Toll-gp83 interaction is unlikely to be a hotspot of reciprocal host-virus adaptation and that other KV genes may be more important in determining host range.

Acknowledgements

We thank Maria-Carla Saleh, Marc Dionne, François Leulier, David Finnegan, and Bruno Lemaitre for kindly sharing RNAi, Toll, and Imd pathway mutant fly lines. We thank Pascale Dijkers, Jean-Luc Imler, Neal Silverman, Edan Foley, and Norbert Perrimon (Addgene plasmid # 37393) for kindly sharing Toll, Imd, and JAK-STAT constructs. We thank Rob Unckless for sharing a DiNV DNA sample with us. We thank the Ruth Steward and the Developmental Studies Hybridoma Bank for making the dorsal antibody available. WHP is supported by the Darwin Trust of Edinburgh and by an EMBO Short-Term Fellowship in RvR's laboratory (Grant Number 7095). Work in RvR's laboratory is supported by a European Research Council Consolidator Grant under the European Union's Seventh Framework Programme (grant number ERC CoG 615680) and a VICI grant from the Netherlands Organization for Scientific Research (grant number 016.VICI.170.090).

References

1. Merkling SH, van Rij RP. 2013. Beyond RNAi: Antiviral defense strategies in Drosophila and mosquito. J Insect Physiol 59:159–170.

2. Xu J, Cherry S. 2014. Viruses and antiviral immunity in Drosophila. Dev Comp Immunol 42:67–84.

3. Bronkhorst AW, van Rij RP. 2014. The long and short of antiviral defense: small RNA-based immunity in insects. Curr Opin Virol 7:19–28.

4. Lamiable O, Imler JL. 2014. Induced antiviral innate immunity in Drosophila. Curr Opin Microbiol 20:62–68.

5. Palmer WH, Varghese FS, van Rij RP. 2018. Natural Variation in Resistance to Virus Infection in Dipteran Insects. Viruses 10:118.

6. Clem RJ. 2001. Baculoviruses and apoptosis: the good, the bad, and the ugly. Cell Death Differ 8:137–143.

7. Bronkhorst AW, van Cleef KWR, Vodovar N, Ince IA, Blanc H, Vlak JM, Saleh M-C, van Rij RP. 2012. The DNA virus Invertebrate iridescent virus 6 is a target of the Drosophila RNAi machinery. Proc Natl Acad Sci 109:E3604–E3613.

8. Kemp C, Mueller S, Goto A, Barbier V, Paro S, Bonnay F, Dostert C, Troxler L, Hetru C, Meignin C, Pfeffer S, Hoffmann JA, Imler J-L. 2013. Broad RNA Interference-Mediated Antiviral Immunity and Virus-Specific Inducible Responses in Drosophila. J Immunol 190:650–658.

9. West C, Silverman N. 2018. p38b and JAK-STAT signaling protect against Invertebrate iridescent virus 6 infection in Drosophila. PLoS Pathog 14:e1007020.

10. Jayachandran B, Hussain M, Asgari S. 2012. RNA interference as a cellular defense mechanism against the DNA virus baculovirus. J Virol 86:13729–34.

11. Webster CL, Waldron FM, Robertson S, Crowson D, Ferrari G, Quintana JF, Brouqui J-M, Bayne EH, Longdon B, Buck AH, Lazzaro BP, Akorli J, Haddrill PR, Obbard DJ. 2015. The Discovery, Distribution, and Evolution of Viruses Associated with Drosophila melanogaster. PLoS Biol 13:e1002210.

12. Bronkhorst AW, van Cleef KWR, Venselaar H, van Rij RP. 2014. A dsRNA-binding protein of a complex invertebrate DNA virus suppresses the Drosophila RNAi response. Nucleic Acids Res 42:12237–48.

13. Bump NJ, Hackett M, Hugunin M, Seshagiri S, Brady K, Chen P, Ferenz C, Franklin S, Ghayur T, Li P. 1995. Inhibition of ICE family proteases by baculovirus antiapoptotic protein p35. Science 269:1885–8.

14. Xue D, Robert Horvitz H. 1995. Inhibition of the Caenorhabditis elegans cell-death protease CED-3 by a CED-3 cleavage site in baculovirus p35 protein. Nature 377:248–251.

15. Byers NM, Vandergaast RL, Friesen PD. 2016. Baculovirus Inhibitor-of-Apoptosis Op-IAP3 Blocks Apoptosis by Interaction with and Stabilization of a Host Insect Cellular IAP. J Virol 90:533–544.

16. Valanne S, Wang J-H, Ramet M. 2011. The Drosophila Toll Signaling Pathway. J Immunol 186:649–656.

17. Myllymaki H, Valanne S, Ramet M. 2014. The Drosophila Imd Signaling Pathway. J Immunol 192:3455–3462.

18. Zambon RA, Nandakumar M, Vakharia VN, Wu LP. 2005. The Toll pathway is important for an antiviral response in Drosophila. Proc Natl Acad Sci 102:7257–7262.

19. Xi Z, Ramirez JL, Dimopoulos G. 2008. The Aedes aegypti toll pathway controls dengue virus infection. PLoS Pathog 4:e1000098.

20. Ramirez JL, Dimopoulos G. 2010. The Toll immune signaling pathway control conserved anti-dengue defenses across diverse Ae. aegypti strains and against multiple dengue virus serotypes. Dev Comp Immunol 34:625–629.

21. Ferreira ÁG, Naylor H, Esteves SS, Pais IS, Martins NE, Teixeira L. 2014. The Toll-Dorsal Pathway Is Required for Resistance to Viral Oral Infection in Drosophila. PLoS Pathog 10:e1004507.

22. Fragkoudis R, Chi Y, Siu RWC, Barry G, Attarzadeh-Yazdi G, Merits A, Nash AA, Fazakerley JK, Kohl A. 2008. Semliki Forest virus strongly reduces mosquito host defence signaling. Insect Mol Biol 17:647–656.

23. Costa A, Jan E, Sarnow P, Schneider D. 2009. The Imd pathway is involved in antiviral immune responses in Drosophila. PLoS One 4:e7436.

24. Avadhanula V, Weasner BP, Hardy GG, Kumar JP, Hardy RW. 2009. A Novel System for the Launch of Alphavirus RNA Synthesis Reveals a Role for the Imd Pathway in Arthropod Antiviral Response. PLoS Pathog 5:e1000582.

25. Waldock J, Olson KE, Christophides GK. 2012. Anopheles gambiae antiviral immune response to systemic O'nyong-nyong infection. PLoS Negl Trop Dis 6:e1565.

26. Sansone CL, Cohen J, Yasunaga A, Xu J, Osborn G, Subramanian H, Gold B, Buchon N, Cherry S. 2015. Microbiota-dependent priming of antiviral intestinal immunity in Drosophila. Cell Host Microbe 18:571–581.

27. Thoetkiattikul H, Beck MH, Strand MR. 2005. Inhibitor B-like proteins from a polydnavirus inhibit NF- B activation and suppress the insect immune response. Proc Natl Acad Sci 102:11426–11431.

28. Lamiable O, Kellenberger C, Kemp C, Troxler L, Pelte N, Boutros M, Marques JT, Daeffler L, Hoffmann JA, Roussel A, Imler J-L. 2016. Cytokine Diedel and a viral homologue suppress the IMD pathway in *Drosophila*. Proc Natl Acad Sci 113:698–703.

29. Bitra K, Suderman RJ, Strand MR. 2012. Polydnavirus Ank proteins bind NF-κB homodimers and inhibit processing of Relish. PLoS Pathog 8:e1002722.

30. Herniou EA, Huguet E, Thézé J, Bézier A, Periquet G, Drezen J-M. 2013. When parasitic wasps hijacked viruses: genomic and functional evolution of polydnaviruses. Philos Trans R Soc Lond B Biol Sci 368:20130051.

31. Mlih M, Khericha M, Birdwell C, West AP, Karpac J. 2018. A virus-acquired host cytokine controls systemic aging by antagonizing apoptosis. PLoS Biol 16:e2005796.

32. Palmer WH, Medd NC, Beard PM, Obbard DJ. 2018. Isolation of a natural DNA virus of Drosophila melanogaster, and characterisation of host resistance and immune responses. PLOS Pathog 14:e1007050.

33. Huger AM. 2005. The Oryctes virus: its detection, identification, and implementation in biological control of the coconut palm rhinoceros beetle, Oryctes rhinoceros (Coleoptera: Scarabaeidae). J Invertebr Pathol 89:78–84.

34. Wang Y, Jehle JA. 2009. Nudiviruses and other large, double-stranded circular DNA viruses of invertebrates: New insights on an old topic. J Invertebr Pathol 101:187–193.

35. Unckless RL. 2011. A DNA Virus of Drosophila. PLoS One 6:e26564.

36. Huger AM. 1985. A new virus disease of crickets (Orthoptera: Gryllidae) causing macronucleosis of fatbody. J Invertebr Pathol 45:108–111.

37. Zelazny B. 1973. Studies on Rhabdionvirus oryctes: II. Effect on adults of Oryctes rhinoceros. J

Invertebr Pathol 22:122–126.

38. Zelazny B. 1972. Studies on Rhabdionvirus oryctes: I. Effect on Larvae of Oryctes rhinoceros and inactivation of the virus. J Invertebr Pathol 20:235–241.

39. Huger AM. 1966. A virus disease of the Indian rhinoceros beetle, Oryctes rhinoceros(Linnaeus), caused by a new type of insect virus, Rhabdionvirus oryctes gen. n., sp. n. J Invertebr Pathol 8:38–51.

40. Parisien J-P, Lau JF, Horvath CM. 2002. STAT2 acts as a host range determinant for species-specific paramyxovirus interferon antagonism and simian virus 5 replication. J Virol 76:6435–41.

41. Mariani R, Chen D, Schröfelbauer B, Navarro F, König R, Bollman B, Münk C, Nymark-McMahon H, Landau NR. 2003. Species-specific exclusion of APOBEC3G from HIV-1 virions by Vif. Cell 114:21–31.

42. Goffinet C, Allespach I, Homann S, Tervo H-M, Habermann A, Rupp D, Oberbremer L, Kern C, Tibroni N, Welsch S, Krijnse-Locker J, Banting G, Kräusslich H-G, Fackler OT, Keppler OT. 2009. HIV-1 antagonism of CD317 is species specific and involves Vpu-mediated proteasomal degradation of the restriction factor. Cell Host Microbe 5:285–97.

43. Rajsbaum R, Albrecht RA, Wang MK, Maharaj NP, Versteeg GA, Nistal-Villán E, García-Sastre A, Gack MU. 2012. Species-specific inhibition of RIG-I ubiquitination and IFN induction by the influenza A virus NS1 protein. PLoS Pathog 8:e1003059.

44. van Mierlo JT, Overheul GJ, Obadia B, van Cleef KWR, Webster CL, Saleh MC, Obbard DJ, van Rij RP. 2014. Novel Drosophila Viruses Encode Host-Specific Suppressors of RNAi. PLoS Pathog 10.

45. Stabell AC, Meyerson NR, Gullberg RC, Gilchrist AR, Webb KJ, Old WM, Perera R, Sawyer SL. 2018. Dengue viruses cleave STING in humans but not in nonhuman primates, their presumed natural reservoir. Elife 7.

46. Lee YS, Nakahara K, Pham JW, Kim K, He Z, Sontheimer EJ, Carthew RW. 2004. Distinct roles for Drosophila Dicer-1 and Dicer-2 in the siRNA/miRNA silencing pathways. Cell 117:69–81.

47. Okamura K, Ishizuka A, Siomi H, Siomi MC. 2004. Distinct roles for Argonaute proteins in small RNA-directed RNA cleavage pathways. Genes Dev 18:1655–66.

48. Weber ANR, Gangloff M, Moncrieffe MC, Hyvert Y, Imler J-L, Gay NJ. 2007. Role of the Spätzle

677 Pro-domain in the Generation of an Active Toll Receptor Ligand. J Biol Chem 282:13522–
678 13531.

679 49. Nusslein-Volhard C. 1979. Maternal effect mutations that affect the spatial coordinates of the
680 embryo of Drosophila melanogaster. Determ Spat Organ 185–211.

681 50. Rutschmann S, Jung AC, Hetru C, Reichhart JM, Hoffmann JA, Ferrandon D. 2000. The Rel
682 protein DIF mediates the antifungal but not the antibacterial host defense in Drosophila.
683 Immunity 12:569–80.

684 51. Anderson K V, Nüsslein-Volhard C. 1984. Information for the dorsal-ventral pattern of the
685 Drosophila embryo is stored as maternal mRNA. Nature 311:223–7.

686 52. Hecht PM, Anderson K V. 1993. Genetic characterization of tube and pelle, genes required for
687 signaling between Toll and dorsal in the specification of the dorsal-ventral pattern of the
688 Drosophila embryo. Genetics 135:405–17.

689 53. Hedengren M, Asling B, Dushay MS, Ando I, Ekengren S, Wihlborg M, Hultmark D. 1999.
690 Relish, a central factor in the control of humoral but not cellular immunity in Drosophila. Mol
691 Cell 4:827–37.

692 54. Pham LN, Dionne MS, Shirasu-Hiza M, Schneider DS. 2007. A Specific Primed Immune
693 Response in Drosophila Is Dependent on Phagocytes. PLoS Pathog 3:e26.

694 55. Hadfield JD. 2010. MCMC Methods for Multi-Response Generalized Linear Mixed Models: The
695 MCMCglmm R Package. J Stat Softw 33:1–22.

696 56. Schindelin J, Arganda-Carreras I, Frise E, Kaynig V, Longair M, Pietzsch T, Preibisch S, Rueden
697 C, Saalfeld S, Schmid B, Tinevez J-Y, White DJ, Hartenstein V, Eliceiri K, Tomancak P, Cardona
698 A. 2012. Fiji: an open-source platform for biological-image analysis. Nat Methods 9:676–682.

699 57. Hill T, Unckless RL. 2017. The dynamic evolution of Drosophila innubila Nudivirus. Infect
700 Genet Evol.

701 58. Tauszig S, Jouanguy E, Hoffmann JA, Imler JL. 2000. Toll-related receptors and the control of
702 antimicrobial peptide expression in Drosophila. Proc Natl Acad Sci U S A 97:10520–5.

703 59. Li Y-X, Dijkers PF. 2015. Specific calcineurin isoforms are involved in Drosophila toll immune
704 signaling. J Immunol 194:168–76.

705 60. Kaneko T, Yano T, Aggarwal K, Lim J-H, Ueda K, Oshima Y, Peach C, Erturk-Hasdemir D,
706 Goldman WE, Oh B-H, Kurata S, Silverman N. 2006. PGRP-LC and PGRP-LE have essential yet

distinct functions in the drosophila immune response to monomeric DAP-type peptidoglycan. Nat Immunol 7:715–723.

61. Foley E, O'Farrell PH. 2004. Functional Dissection of an Innate Immune Response by a Genome-Wide RNAi Screen. PLoS Biol 2:e203.

62. Baeg G-H, Zhou R, Perrimon N. 2005. Genome-wide RNAi analysis of JAK/STAT signaling components in Drosophila. Genes Dev 19:1861–1870.

63. van Cleef KWR, van Mierlo JT, van den Beek M, van Rij RP. 2011. Identification of Viral Suppressors of RNAi by a Reporter Assay in Drosophila S2 Cell Culture, p. 201–213. *In* Methods in molecular biology (Clifton, N.J.).

64. Werner T, Borge-Renberg K, Mellroth P, Steiner H, Hultmark D. 2003. Functional diversity of the Drosophila PGRP-LC gene cluster in the response to lipopolysaccharide and peptidoglycan. J Biol Chem 278:26319–22.

65. Van Cleef KWR, Van Mierlo JT, Miesen P, Overheul GJ, Fros JJ, Schuster S, Marklewitz M, Pijlman GP, Junglen S, Van Rij RP. 2014. Mosquito and Drosophila entomobirnaviruses suppress dsRNA- and siRNA-induced RNAi. Nucleic Acids Res 42:8732–8744.

66. Smits AH, Jansen PWTC, Poser I, Hyman AA, Vermeulen M. 2013. Stoichiometry of chromatin-associated protein complexes revealed by label-free quantitative mass spectrometry-based proteomics. Nucleic Acids Res 41:e28–e28.

67. Cox J, Mann M. 2008. MaxQuant enables high peptide identification rates, individualized p.p.b.-range mass accuracies and proteome-wide protein quantification. Nat Biotechnol 26:1367–1372.

68. Tyanova S, Temu T, Sinitcyn P, Carlson A, Hein MY, Geiger T, Mann M, Cox J. 2016. The Perseus computational platform for comprehensive analysis of (prote)omics data. Nat Methods 13:731–740.

69. Mackay TFC, Richards S, Stone EA, Barbadilla A, Ayroles JF, Zhu D, Casillas S, Han Y, Magwire MM, Cridland JM, Richardson MF, Anholt RRH, Barrón M, Bess C, Blankenburg KP, Carbone MA, Castellano D, Chaboub L, Duncan L, Harris Z, Javaid M, Jayaseelan JC, Jhangiani SN, Jordan KW, Lara F, Lawrence F, Lee SL, Librado P, Linheiro RS, Lyman RF, Mackey AJ, Munidasa M, Muzny DM, Nazareth L, Newsham I, Perales L, Pu L-L, Qu C, Ràmia M, Reid JG, Rollmann SM, Rozas J, Saada N, Turlapati L, Worley KC, Wu Y-Q, Yamamoto A, Zhu Y, Bergman CM, Thornton KR, Mittelman D, Gibbs RA. 2012. The Drosophila melanogaster

738 Genetic Reference Panel. Nature 482:173–8.

739 70. Li H, Li WX, Ding SW. 2002. Induction and Suppression of RNA Silencing by an Animal Virus.
740 Science (80-) 296:1319–1321.

741 71. Van Rij RP, Saleh MC, Berry B, Foo C, Houk A, Antoniewski C, Andino R. 2006. The RNA
742 silencing endonuclease Argonaute 2 mediates specific antiviral immunity in Drosophila
743 melanogaster. Genes Dev 20:2985–2995.

744 72. Nayak A, Berry B, Tassetto M, Kunitomi M, Acevedo A, Deng C, Krutchinsky A, Gross J,
745 Antoniewski C, Andino R. 2010. Cricket paralysis virus antagonizes Argonaute 2 to modulate
746 antiviral defense in Drosophila. Nat Struct Mol Biol 17:547–554.

747 73. van Mierlo JT, Bronkhorst AW, Overheul GJ, Sadanandan SA, Ekström J-O, Heestermans M,
748 Hultmark D, Antoniewski C, van Rij RP. 2012. Convergent evolution of argonaute-2 slicer
749 antagonism in two distinct insect RNA viruses. PLoS Pathog 8:e1002872.

750 74. Dostert C, Jouanguy E, Irving P, Troxler L, Galiana-Arnoux D, Hetru C, Hoffmann JA, Imler JL.
751 2005. The Jak-STAT signaling pathway is required but not sufficient for the antiviral response
752 of drosophila. Nat Immunol 6:946–953.

753 75. Arbouzova NI, Zeidler MP. 2006. JAK/STAT signalling in Drosophila: insights into conserved
754 regulatory and cellular functions. Development 133:2605–16.

755 76. Wang Y, Kleespies RG, Huger AM, Jehle JA. 2007. The genome of Gryllus bimaculatus
756 nudivirus indicates an ancient diversification of baculovirus-related nonoccluded nudiviruses
757 of insects. J Virol 81:5395–406.

758 77. Zhao J, He S, Minassian A, Li J, Feng P. 2015. Recent advances on viral manipulation of NF-κB
759 signaling pathway. Curr Opin Virol 15:103–11.

760 78. Zehavi Y, Sloutskin A, Kuznetsov O, Juven-Gershon T. 2014. The core promoter composition
761 establishes a new dimension in developmental gene networks. Nucleus 5:298–303.

762 79. Obbard DJ, Gordon KHJ, Buck AH, Jiggins FM. 2009. The evolution of RNAi as a defence
763 against viruses and transposable elements. Philos Trans R Soc Lond B Biol Sci 364:99–115.

764 80. Sawyer SL, Elde NC. 2012. A cross-species view on viruses. Curr Opin Virol 2:561–8.

765 81. Brockhurst MA, Chapman T, King KC, Mank JE, Paterson S, Hurst GDD. 2014. Running with the
766 Red Queen: the role of biotic conflicts in evolution. Proc R Soc London B Biol Sci 281.

82. Nitta KR, Jolma A, Yin Y, Morgunova E, Kivioja T, Akhtar J, Hens K, Toivonen J, Deplancke B, Furlong EEM, Taipale J. 2015. Conservation of transcription factor binding specificities across 600 million years of bilateria evolution. Elife 4.

83. Guindon S, Dufayard J-F, Lefort V, Anisimova M, Hordijk W, Gascuel O. 2010. New Algorithms and Methods to Estimate Maximum-Likelihood Phylogenies: Assessing the Performance of PhyML 3.0. Syst Biol 59:307–321.

Figure legends

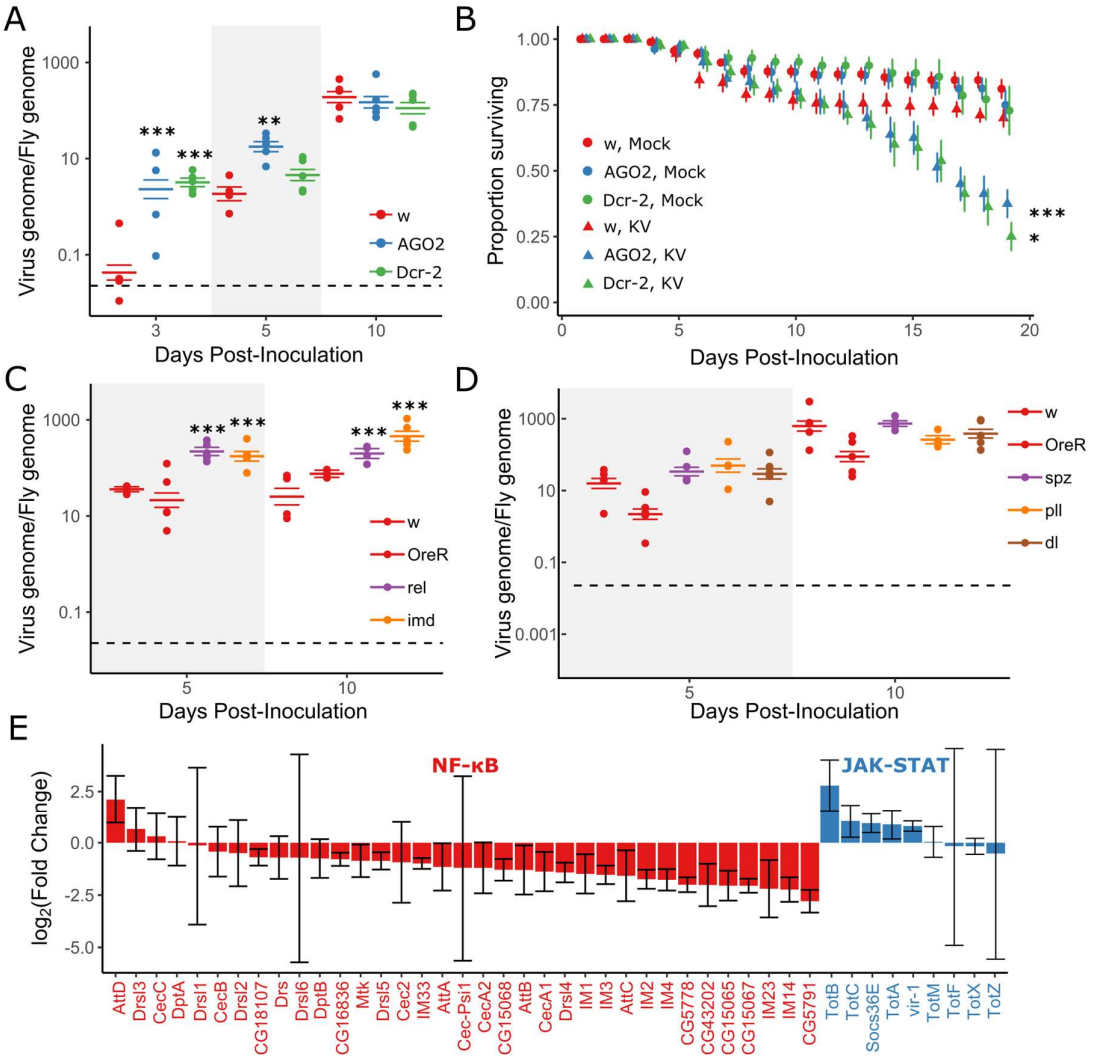

Figure 1: RNAi and Imd pathways provide antiviral defense against Kallithea virus

Mutants for RNAi (A,B) and NF-κB (C,D) pathways were assayed for viral titre (A,C,D) and mortality (B) following KV infection. OreR and w^{1118} flies were used as wild-type controls. Viral titre was measured by qPCR, relative to Rpl32 DNA, where each data point represents a vial of 5 flies, and coloured horizontal lines correspond to the mean titre and associated standard error (A,C,D). Horizontal dotted lines (A,C,D) represent the amount of virus injected. (B) RNAi mutants (*AGO2* and *Dcr2*) and w^{1118} controls were injected with chloroform-treated KV (mock) or KV, and survival was

monitored each day. Each point is the mean number of surviving flies across 10 vials of 10 flies, with associated standard errors. (E) Log-transformed fold changes of presumed NF-κB-responsive genes (coloured red - *Cecropins*, *Diptericins*, *Attacins*, *Metchnikowin*, *Drosomycins* and *Drosomycin-like* genes, Bomamins (i.e. *IM1*, *CG18107*, *IM2*, *IM3*, *CG15065*, *CG15068*, *CG43202*, *CG16836*, *CG5778*, *IM23*, *CG15067*, *CG5791*), and other IM genes) and JAK-STAT-responsive genes (coloured blue - *Socs36E*, v*ir-1*, and *Turandot* (*Tot*) family) following KV infection of *OreR* flies at 3 dpi, relative to uninfected controls (ERP023609; n = 5 libraries per treatment, with n=10 flies per library (32)). Error bars show standard errors of the mean. *p < 0.05; **p < 0.01; ***p < 0.001 (Statistical tests performed in MCMCglmm).

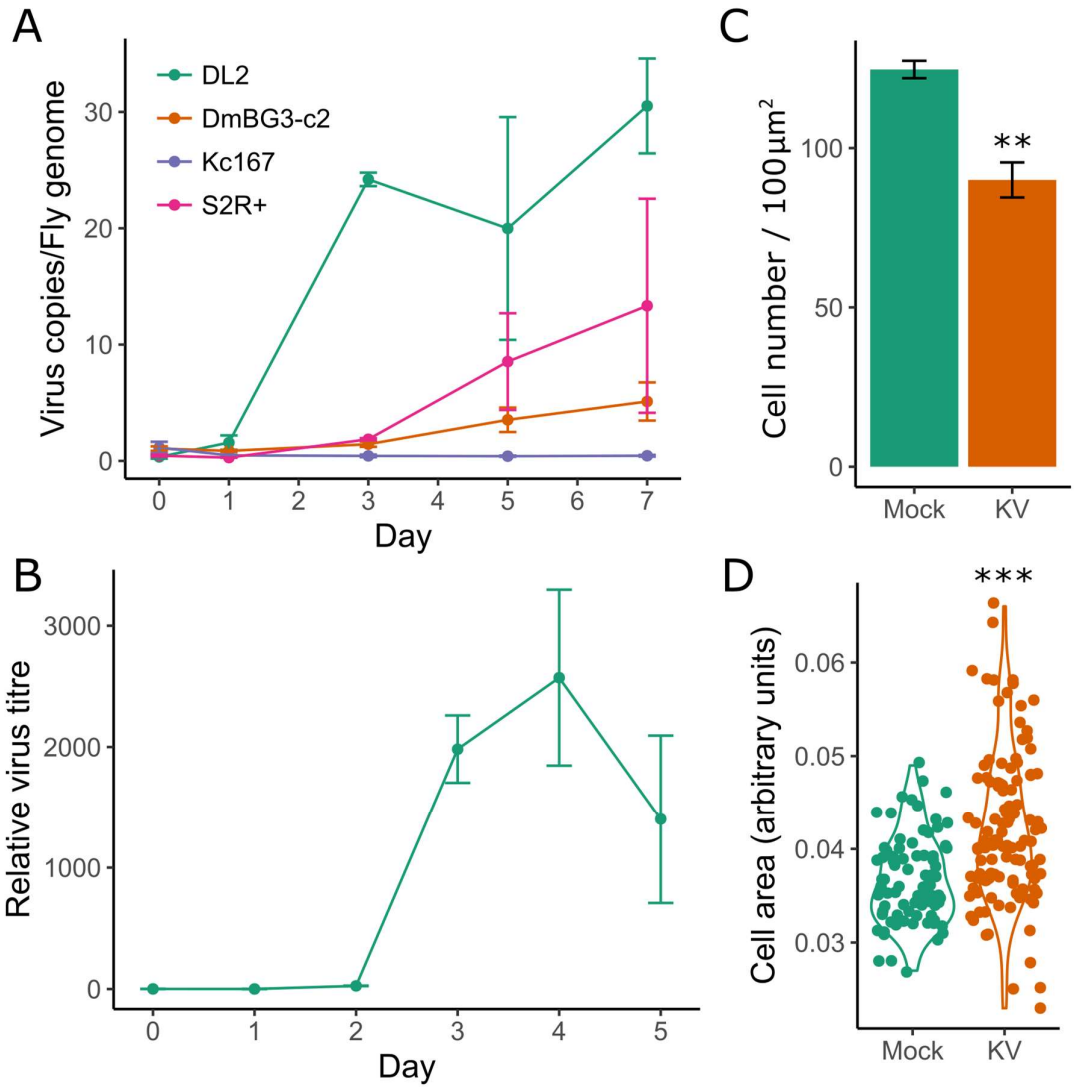

Figure 2: KV replicates in cell culture

KV growth was assessed in various *D. melanogaster* cell lines by qPCR against the KV genome, relative to the fly gene Rpl32 (n=3 for each time point). (B) KV release from S2 cells into the culture medium was assessed by DNA extraction of 50 µL of culture medium and qPCR against the KV genome, plotted relative to the amount of KV in the medium directly following infection (i.e. zero time point is equal to 1). (C) Cell density (number of cells per approximately 100 μm^2 in KV versus mock-treated cells) at 10 dpi (n=3). (D) Cell size of mock or KV-infected cells at 10 dpi. Each dot represents a single cell and the data distribution is presented as a violin plot. Error bars show standard error of the mean. *p < 0.05; **p < 0.01; ***p < 0.001 (Statistical tests performed in MCMCglmm)

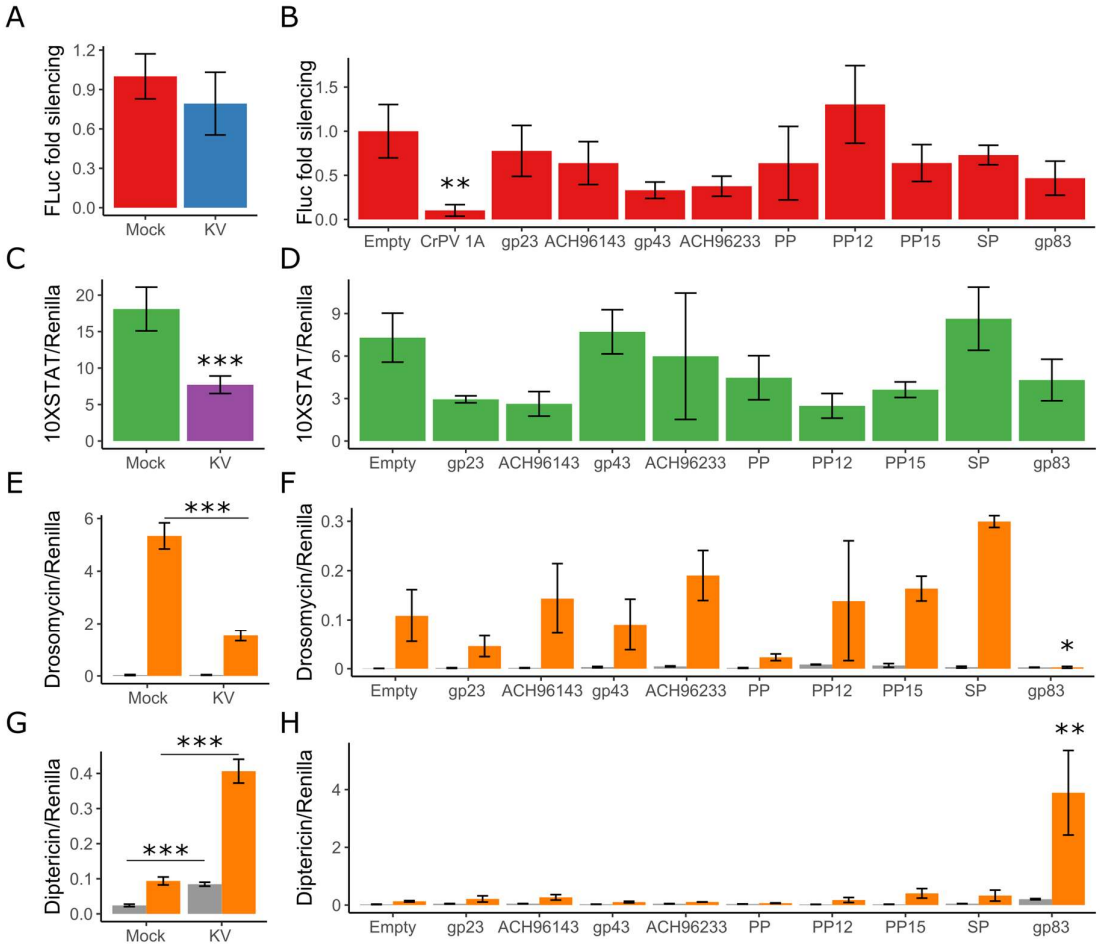

Figure 3: Kallithea virus gp83 suppresses Toll and induces Imd signalling

The ability of KV (4 dpi) and 9 highly expressed KV genes to inhibit RNAi (A,B), JAK-STAT (C,D), Toll (E,F), and Imd (G,H) pathways was assessed. For RNAi suppression assays (A,B), RNAi efficiency was assessed by transfecting S2 cells with expression plasmids expression FLuc and, as a normalization control RLuc, along with dsRNA targeting either FLuc or GDP. Data are expressed as fold silencing in cells treated with GFP dsRNA relative to those treated with FLuc dsRNA, normalised to 1 in mock-infected cells. The CrPV suppressor of RNAi, protein 1A, was used as a positive control (data combined from 2 experiments). For JAK-STAT suppression assays (C,D), S2 cells were transfected with a plasmid encoding FLuc under control of 10 STAT binding sites (10XSTAT-FLuc). In contrast to the JAK-STAT pathway, the Toll and Imd pathways are not endogenously active in S2 cells (grey bars in E, F, G, H), but can be activated by expression of $Toll^{LRR}$ (orange bars in E, F) or PGRP-LC (orange bars in G, H). For Toll suppression assays (E,F), S2 cells were transfected with the Drs-FLuc reporter, encoding FLuc under control of a *Drosomycin* promoter, with either pAc5.1-$Toll^{LRR}$ or an empty control plasmid (grey bars) For Imd suppression assays (G,H), S2 cells were transfected with the Dpt-FLuc reporter, encoding FLuc under control of a *Diptericin* promoter, with either pMT (Empty) or pMT-PGRP-LC. All FLuc luciferase values were normalized to Renilla luciferase (RLuc) values, driven by a constitutively active *Actin* promoter from a co-transfected plasmid. PP=Putative Protein; SP=Serine Protease. Error bars show standard errors of the mean, calculated from 5 biological replicates for (A,C,E,G) and at least 3 biological replicates for (B,D,F,H). *$p < 0.05$; **$p < 0.01$; ***$p < 0.001$ (Statistical tests performed in MCMCglmm).

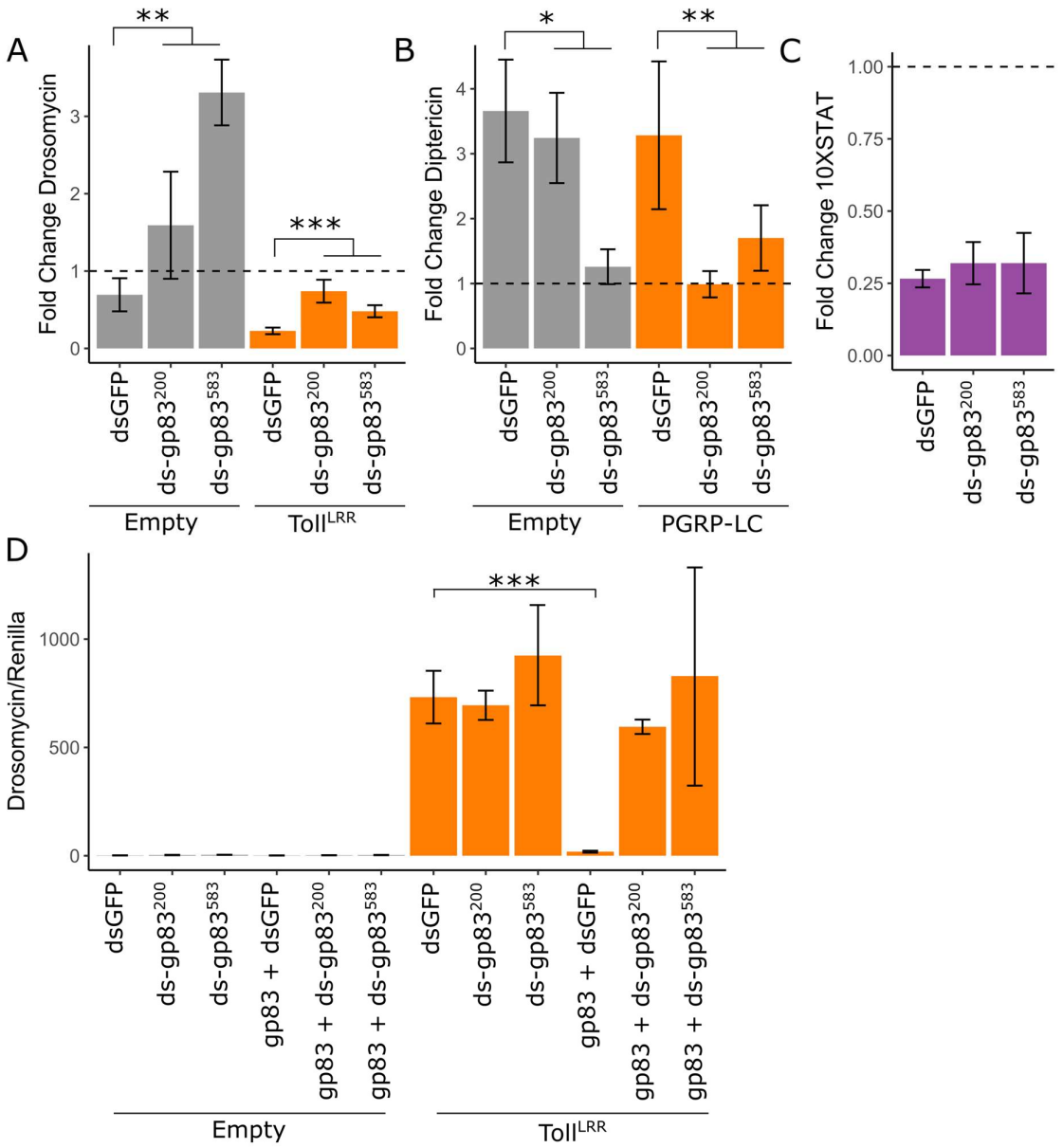

835

836 *Figure 4: KV induction and suppression of NF-KB pathways is mediated by gp83*

837 The ability of KV to inhibit Toll (A), induce Imd (B), and inhibit JAK-STAT (C) was assessed during gp83

838 knockdown, using two independent dsRNAs against gp83 (labelled ds-gp83^{200} and ds-gp83^{583}).

839 Drosomycin, diptericin, and 10X-STAT activity was measured as Drs-FLuc, Dpt-FLuc, and 10XSTAT-

840 FLuc expression, relative to RLuc expression as described in the legend to Figure 3. For each, data are

841 presented as fold change in signalling following KV infection relative to mock infection (chloroform

842 treated KV) (4 dpi), where 1 (horizontal dotted line) represents no induction or suppression of the
843 pathway by KV infection. (A) Fold change in Drs-FLuc expression following KV infection of S2 cells
844 with (orange bars) or without (grey bars) activation of the pathway by $Toll^{LRR}$ expression. (B) Fold
845 change in Dpt-FLuc expression following KV infection of S2 cells with (orange bars) or without (grey
846 bars) pathway activation by PGRP-LC expression. (C) Fold change in 10X-STAT FLuc expression
847 following KV infection of S2 cells. (D) Efficiency of gp83 knockdown was assessed by co-transfection
848 of an expression plasmid encoding gp83 with two independent dsRNAs against gp83 and Drs-FLuc
849 reporter plasmids. Error bars show standard error of the mean (A-C: n = 5 biological replicates, D: n =
850 3 biological replicates). *$p < 0.05$; **$p < 0.01$; ***$p < 0.001$ (Statistical tests performed in
851 MCMCglmm).

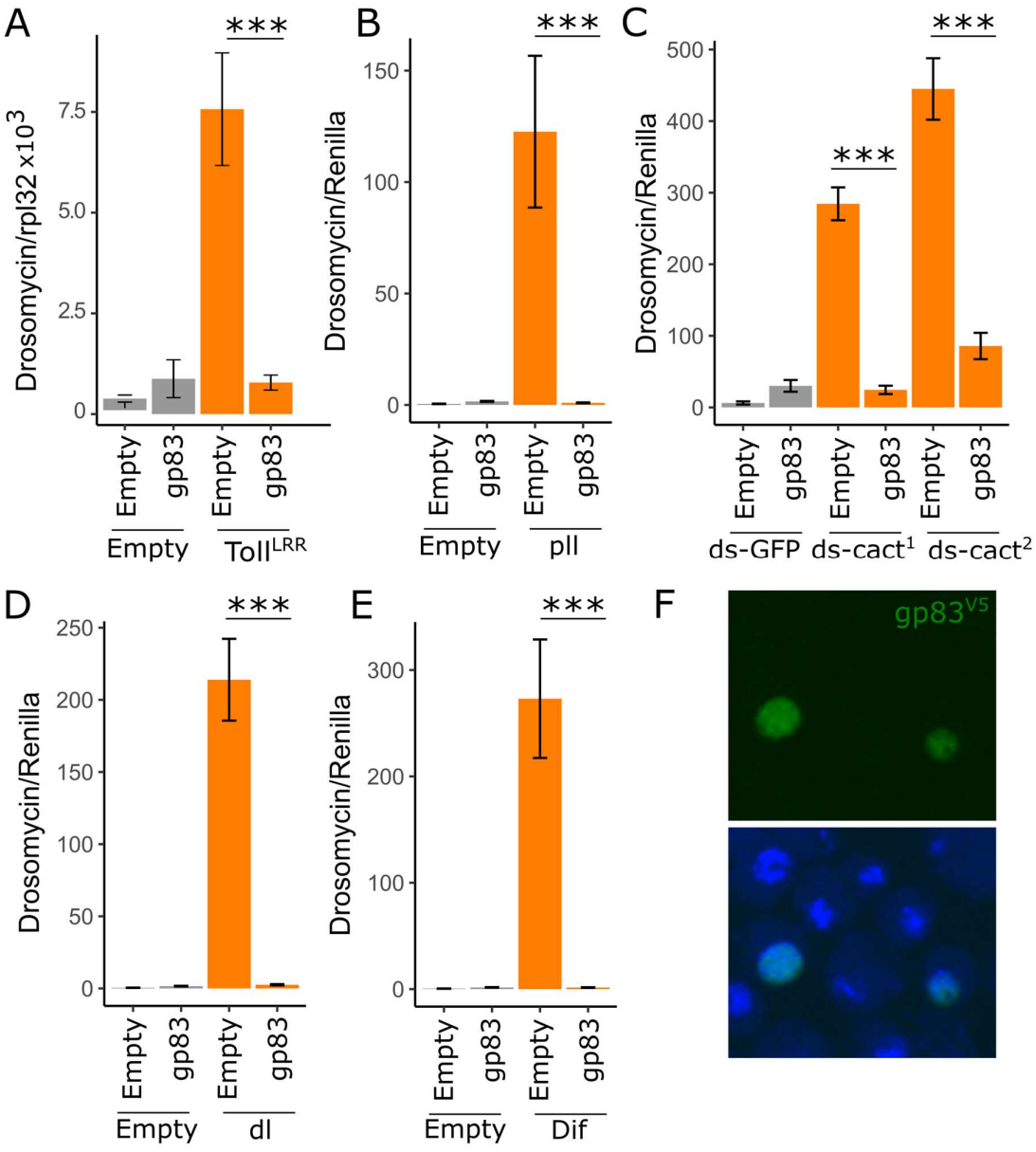

852

853 *Figure 5: gp83 inhibits Toll signalling downstream of Dif and dorsal*

854 (A) The ability to of gp83 to inhibit endogenous *Drosomycin* expression was assessed by transfection
855 of S2 cells with pAc-gp83 or empty control plasmid, and the Toll pathway was activated by
856 cotransfection of pAc-Toll^{LRR} or control plasmid. *Drosomycin* expression levels were measured
857 relative to *Rpl32* expression by qRT-PCR. (B-E) The Toll pathway was activated downstream of the
858 Toll receptor by transfection of a plasmid encoding *pll* (B), knockdown of *cactus* with two

859 independent, non-overlapping dsRNAs (labelled ds-cact^{1} and ds-cact^{2}) (C), and transfection of
860 plasmids encoding the transcription factors *dl* and *Dif* (D,E). Activation of the pathway was assessed
861 using the Drs-FLuc reporter, relative to RLuc expression (orange bars in B-E; grey bars represent
862 controls in which empty plasmids (B, D, E) or dsRNA targeting GFP (C) were transfected). Suppression
863 of the Toll pathway at different stages by gp83 was assessed by co-transfection of pAc-gp83 or an
864 empty control plasmid (B-E). (F) Representative confocal image of S2 cells expressing V5 epitope-
865 tagged gp83 stained with a V5 antibody (upper panel) and a merged image in which nuclei are
866 stained with Hoechst (lower panel). Error bars show standard error of the mean (n = 5 biological
867 replicates). *$p < 0.05$; **$p < 0.01$; ***$p < 0.001$ (Statistical tests performed in MCMCglmm).

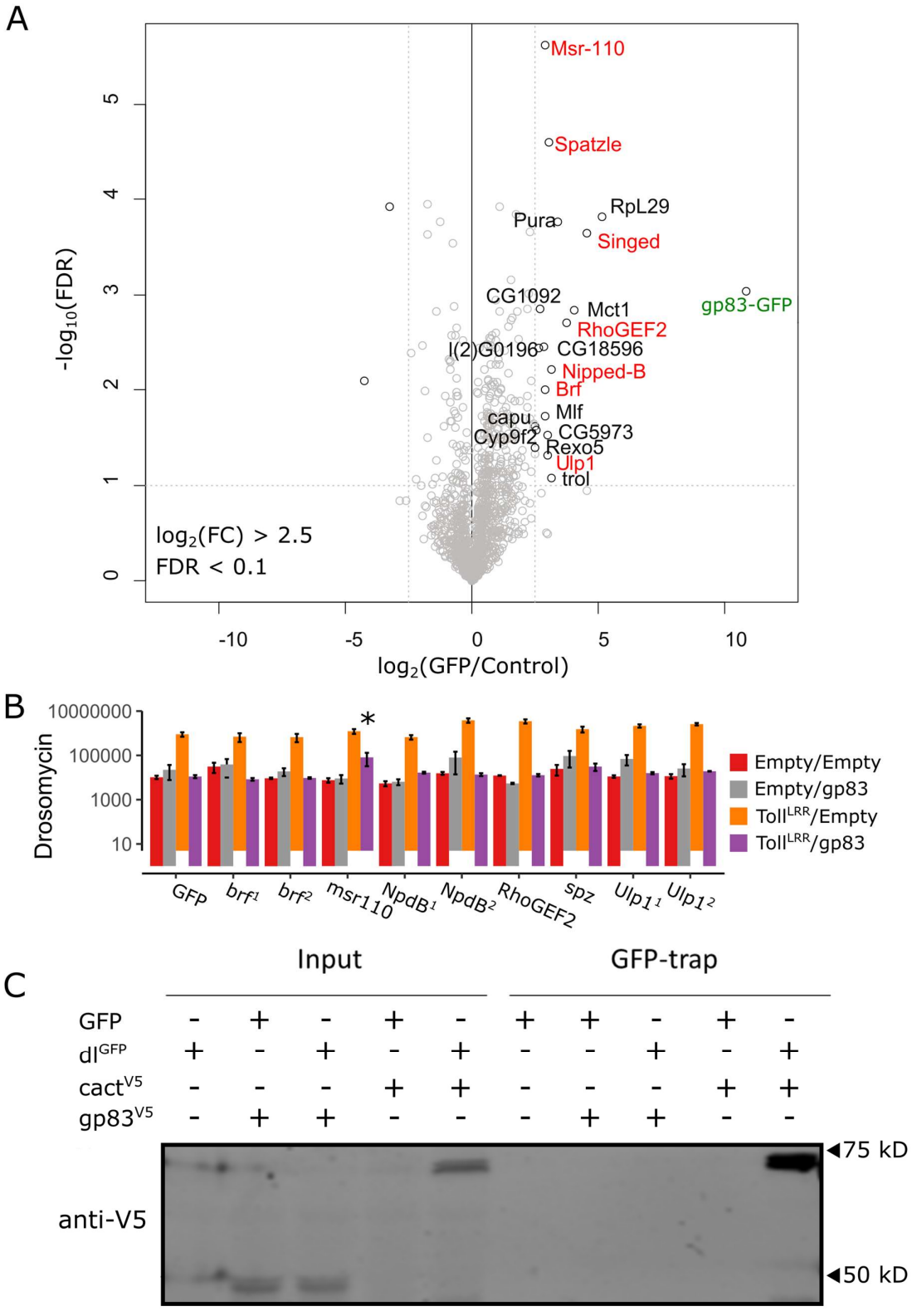

Figure 6: Identification of host interactors of gp83

(A) Identification of gp83 interacting proteins in S2 cell lysates by label-free quantitative (LFQ) mass spectrometry. Permutation-based FDR-corrected t-tests were used to determine proteins that are statistically enriched in gp83-GFP immunoprecipitated (IP). The $\log_2$ LFQ intensity of gp83-GFP IP over control IP (cells that do not express gp83-GFP) is plotted against the $-\log_{10}$ FDR. The gp83-GFP bait (labelled in green) and interactors with an enrichment of fold change > 2.5; $-\log_{10}$ FDR > 1 are indicated. (B) Drs-FLuc expression was measured following co-transfection of pAc-gp83, pAc-Toll^{LRR}, or empty control plasmids, along with dsRNA targeting *brf*, *msr-110*, *Nipped-B*, *RhoGEF2*, *spatzle*, and *Ulp1* (labelled red in panel A), with dsRNA targeting GFP as a control. Genes are superscripted with '1' or '2' when two independent dsRNAs were used to knock down the gene. Although *msr-110* kncockdown appears to partially rescue gp83 immunosuppression, subsequent experiments did not reproduce this effect. Error bars represent standard error of the mean (n=3). Statistical tests were performed in MCMCglmm. (C) V5-tagged gp83 or V5-tagged cact (an IκB protein known to interact with dl) were expressed alongside GFP-tagged dl or GFP and GFP-associated complexes were immunoprecipitated (IP) with GFP-trap magnetic beads and analyzed by western blot using V5 antibodies. Note, cact appears to be stabilized when co-expressed with dl compared to when it is expressed alone.

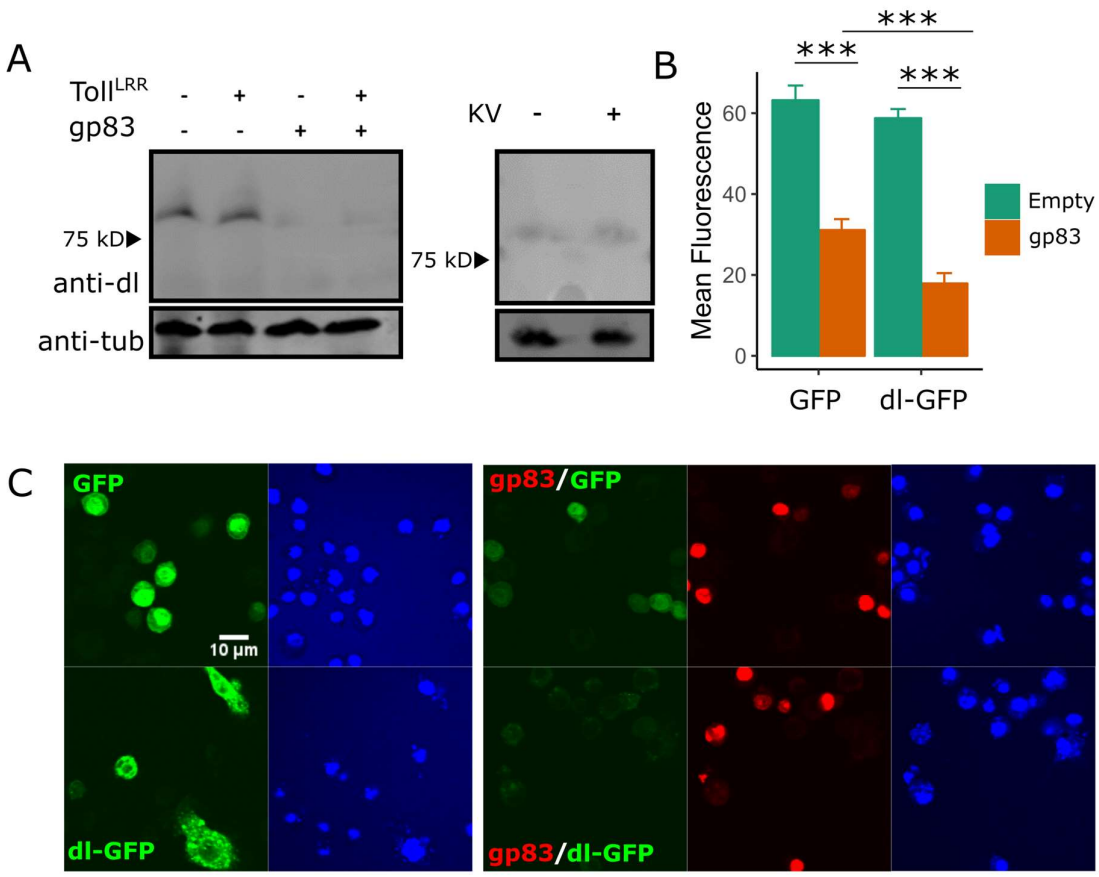

Figure 7: Overexpression of gp83 may reduce dorsal levels

(A) Western blots show endogenous dl protein levels in S2 cells transfected with a plasmid encoding gp83 or empty control plasmid (left panel) and in S2 cells infected with KV (4 dpi) (right panel). The Toll pathway was activated by expression of pAc-Toll^{LRR}, as indicated. Western blot analysis using anti-Tubulin antibody was used to very equal loading. . (B-C) The effect of gp83 was analyzed by confocal microscopy of S2 cells transfected with plasmid encoding gp83 or control plasmid, and plasmids encoding either GFP or dl-GFP. ImageJ-based quantification of mean GFP fluorescence for individually outlined cells (n ≥ 20 cells for each condition, error bars show standard error of the mean). (C) A representative image from (B), showing GFP (top panels) and dl-GFP expression (lower panels) with or without gp83. Nuclei were visualized using Hoechst ***p < 0.001.

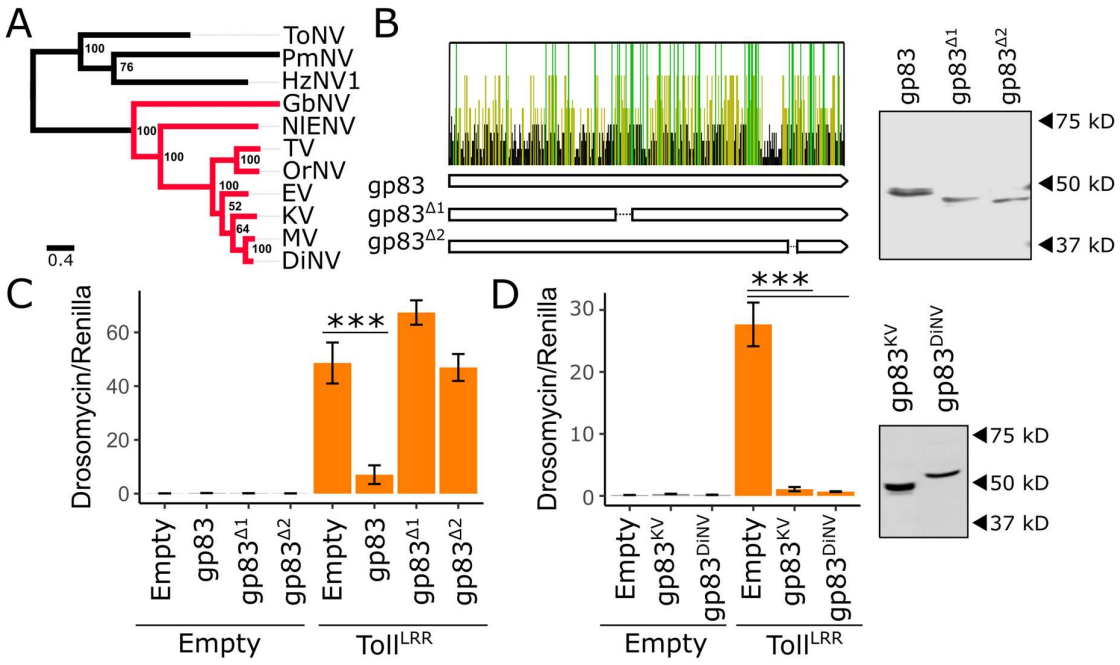

897

898 *Figure 8: The immunosuppressive function of gp83 is evolutionarily conserved*

899 (A) Maximum likelihood phylogeny inferred from a protein alignment of nudivirus-encoded DNA
900 polymerase B using PhyML (83), with an LG substitution model and gamma-distributed rate
901 parameter. Support for each node was assessed by bootstrapping, and the scale bar represents
902 substitutions per site. Nudivirus species that encode gp83 homologs are coloured in red. (B)
903 Conservation of the gp83 amino acid sequence across 7 species of nudivirus (all red labelled viruses
904 in panel A, except the endogenized virus NlENV). Each bar represents an amino acid, and bars are
905 coloured yellow if the residue is conserved in ≥ 50% of the species, green if conserved in 100% of the
906 species., and black if conserved in <50% of the species. Two V5-tagged gp83 constructs were created
907 with deletionsthat span regions with an excess of conserved residues: gp83$^{\Delta1}$ and gp83$^{\Delta2}$. Western
908 blot and subsequent V5 antibody staining show that both deletion constructs accumulate to similar
909 levels as full-length gp83 following transfection of S2 cells. (C) Full-length gp83, gp83$^{\Delta1}$, or gp83$^{\Delta2}$
910 were co-expressed with Toll^{LRR}, and Drs-FLuc expression was measured relative to pAct-FLuc
911 expression. (D) V5-tagged gp83 from KV and DiNV were co-expressed with Toll^{LRR} to assess
912 suppression of Drs-FLuc expression (relative to pAct-FLuc expression) in *D. melanogaster* S2 cells.

913 Western blot analyses using V5 antibody was usedto confirm gp83 expression. Error bars show
914 standard error of the mean (n = 5 biological replicates). *p < 0.05; **p < 0.01; ***p < 0.001
915 (Statistical tests performed in MCMCglmm).

916